SCINTILLATOR WAVELENGTH INFLUENCE IN AN OPTICAL DOSIMETER

Master of Medical Physics

Department of Physics and Astronomy

University of Canterbury

Christchurch

New Zealand

2006

By

Tom Chien-Sheng Chen

TABLE OF CONTENT

FIGURES CONTENT

TABLE CONTENT

ABSTRACT

Green and red scintillator crystals with plastic fiber optics were used to investigate their application as optical fiber dosimeters. In Part 1, the radiation beam is perpendicular to the system with 20x20cm^2 half field. We have a linear response for both systems with doubling the MU starting from 1MU up to 1024MU. Here we define the SOBR (Signal to Optical Background Ratio) to be the response of total signal (crystal and fiber) divided by the background (fiber) signal. The SOBR of red and green with no filter were 16.58 and 17.74 respectively. When we added the filter, the SOBR for red and green became 11.03 and 66.72 respectively. In Part 2, we changed the field to X=1cm, Y1=5cm and Y2=1cm. The SOBR for red and green with no filter are 44.43 and 45.47. After we added the filter, the SOBR for red and green became 15.62 and 1684. This change in field shape gave us a higher SOBR, especially when the filter was added. In Part 3, we tested the angular response of our detector. Both systems increased their response when gantry angle reach 45° and -45° (315°). When the filter was added, a change of a factor of 2 in response remained. When the crystal was then rotated and pointed in the direction of the gantry, good response was obtained from range 90° to -90° (270°). The response of green system was within 2.5%. For the red system, a large step about 10% was observed. Conversion of the fiber fluorescence and Cerenkov radiation in the scintillator crystal and transmission to the detector is a problem in all optical fiber systems, including the dual fiber system, that remains to be addressed.

INTRODUCTION

In medical practice, many different detectors have been introduced and produced in the areas of radiotherapy, stereotactic radiosurgery and any related fields. An ionising chamber has always been the ideal detector for set ups and quality assurance for linear accelerators [1]. But people have discovered that ionising chambers actually have many limitations and problems. For example, its size and accuracy during use in other areas like IMRT. In IMRT, a high dose in a small area is often the case of treatment. Therefore, high accuracy and small size detectors with high spatial resolution would be ideal for this situation [2-4]. Reports have shown that dose discrepancies can go as high as 10% during use of standard ionising chambers between the cross-profile of an intensity modulated beam and planned values [5]. This is caused by the averaging effect of the detectors due to their relatively large detecting volumes [6,7].

In therapeutic situations, one of the detectors that can be used in real time is TLD. This is a kind of scintillation detector which traps the electrons in the excited state after interaction with ionising radiation. To "read" the TLD, it needs to be heated in front of a PMT. This heat energy will bring the trapped electron back to the ground state and light will be given off [8]. This whole procedure is very time consuming and does not give us readings in real time. Therefore, this scintillation dosimeter is not ideal for radiotherapy or stereotactic radiosurgery.

Scintialltion dosimetry is a very good method for making detectors. Organic scintillators are simple and small in size with instant light given off and high spatial resolution. Other advantages includes no temperature, pressure or humidity corrections required [9, 10]. Many people have tried many different experiments to discover the best way of building a scintillator detector.

Until now, even though we still haven't got a final drawing of this new scintillator detector, people are starting to understand more about scintillation dosimetry and the problems and difficulties involved [9, 11-16]. The basic components of a scintillator detector are detector probe, light guide and a photo detector [1]. The detector probe can be made from scintillating fiber, plastic scintillator or even scintillator sheets [1, 17, 18].

A light guide is used to transport light signals from the detector probe to the photo detector. The best light guide to use is optical fiber. Photodiodes and photomultiplier tube (PMT) are two good choices of photo detector [11]. Photodiodes have been the best choice for scintillator detectors due to their simplicity, good reproducibility and stability response and the ability to perform absolute dosimetry [19, 20]. Later, people discovered during the interaction of scintillator dosimeter and ionizing radiation, two forms of light signals are produced. They are Cerenkov radiation and fluorescence.

Cerenkov radiation occurs when secondary electrons pass through a translucent material faster than light travels in that material [9]. It has a continuous spectrum that spans from the ultraviolet to infrared regions and varies with magnitude according to λ^{-3} [9, 10]. Therefore, Cerenkov radiation is stronger in the UV and the blue region of the visible spectrum than in the infrared [9]. Cerenkov radiation is actually the predominant noise of scintillator detectors. Fluorescence on the other hand, is estimated to be 5% of the Cerenkov radiation contribution with incident 20 MeV electrons [9, 21]. Fluorescence emission is isotropic [21], unlike Cerenkov radiation. The intensity of fluorescence is related to the impurity concentration of the light guide [9, 22].

These two types of unwanted light will affect the accuracy of the scintillator detector. So removing them as much as possible is an essential thing to do. Scientists and physicists have tried different ways to eliminate these two unwanted signals [23-24]. Some results are better than others. To this day, people are still doing experiments and trying to find the best possible way to completely eliminate Cerenkov radiation and fluorescence from the scintillation.

In 1999 D. Létourneau [19] and his team designed a detector consisting of two identical 10m optical fibers. One fiber has a scintillating fiber attached to it, the other one is just a fiber which acts as a reference fiber. Each fiber is connected to a photodiode and then electrometer and computer for current measurement and voltage conversion. What D. Létourneau had in mind was that when radiation interacts with both fibers, the one with scintillating fiber will give him the main signal plus the background signal.

The background signal will of course be the Cerenkov and the fluorescence. The reference fiber will only give him the background signal, because no scintillating fiber is attached. So by subtracting the reference signal from the scintillation fiber signal, he can have the signal with both Cerenkov and fluorescence eliminated.

The problems that he faced were ambient light infiltration, electromagnetic fields and the internal noise of the system itself which are inherent. But he managed to solve these problems by covering up the scintillating fiber and also by using paint. This will prevent light entering into the system. He placed a copper shielding around the photodiode to minimize or even eliminate the electromagnetic field. But he also suggested some other ways to improve his detector. That is by keeping the photodiode temperature at 10°, which will reduce the internal noise. His system is mainly to be used for quality assurance of the LINAC such as measuring, depth dose cures and beam profiles etc. It is also good for a field size greater than 2cm diameter.

In 2004 Louis Archambault [1] and his team designed a system to compare scintillating fiber with scintillator crystal. He used four different scintillating fibers and two different plastic scintillators. They all attached to an optical fiber. The wavelength Louis dealt with in his research was in the range 423nm to 530nm. That is from blue to about orange. The main purpose of his research was to see which type of scintalltor gives optimum signal. He also looked at the response of different lengths and diameters of the scintillators and scintillating fibers. He concluded that scintillating fiber behaves better than the plastic scintillating fiber, because overall, they produce more light than the plastic scintillator.

In 2003, A Sam Beddar and his team [25] investigated the behavior of Cerenkov radiation by using scintillating fiber with optical fiber.
They wanted to understand the behavior of Cerenkov so they could work out a way to minimise its capture. The main area that they have looked at was the refractive index of the fiber. The fiber contains two different refractive indices, one for core and one for cladding. He discovered that the differences of core and cladding refractive index will affect the amount of Cerenkov been captured. The lower the refractive index difference between the core and the cladding, the less Cerenkov will get captured. But this will also reduce the acceptance angle of the fiber, which will allow less

scintillation signal from the scintillator to reach the photo detector. The way to solve this problem is by increasing the size of the fiber which will increase the size of fiber core, so more light can enter the fiber and be transmitted to the photo detector. But by increasing the size of the fiber, the amount of Cerenkov generated in the core will also increase. So this became a problem.

In 1999, M A Clift and his team [9] used plastic scintillators with optical fiber to investigate ways to enhance light signal and also to eliminate the Cerenkov radiation. They used red and green plastic scintillators from Bicron and did experiments with different reflective paint and coatings on the plastic scintillators to increase the light signals reaching the photodiode. They've also tried different types of optical filters to filtrate Cerenkov and fluorescence in the system.

All those people mentioned above have tried to do their best to accomplish the mission of "more scintillation signal and less background signal". They've all achieved different results. Those results can really help people in the future who want to do further studies on this topic. There are various places in the system that can be improved. Different manufacturers are developing parts that perform better than their predecessors. Also, different experiment set ups can be considered to achieve an optimum result. In my research project, that is exactly what we are trying to do. By using different plastic scintillators and set ups, we see how our result compares with the work that has been previously done. Mohammad Ali Alhabdan, a student of doctorate of philosophy in medical physics of University of Canterbury, New Zealand, did his research on "Dosimeters Using Plastic Scintillators and Fiber Optics" [26]. He used a blue plastic scintillator crystal that emitted 425nm wavelength of light. He has achieved a very good result with his designed system and scintillator.

What we want to do is use his system but with red and green light emitting plastic scintillators, to see if this will further improve the system.

MATERIAL & METHODS

To perform the measurements for this experiment, the following equipment was required:

- ✓ Linear Accelerator
- ✓ Scintillator Crystal
- ✓ Optical Fiber
- ✓ Lenses
- ✓ Optical Filter
- ✓ Photodiode
- ✓ Electronic Integrator

Linear Accelerator

We used a Varian 600 C Linear Accelerator in the Treatment 3 room of the Oncology Department in Christchurch Public Hospital CDHB. Varian 600C is a single energy linear accelerator. It can only generate a 6 M.V. single energy beam. No other energies can be generated. Electron beams are not available with the Varian 600 C, only photon beams. The dose rate for this machine is measured in monitoring unit (MU). The range of the monitoring units for 600 C is from 50 MU per minute to 250 MU per minute.

Scintillator Crystal

Two different scintillator crystals were selected to perform this research project, a red crystal that emits light with a wavelength of 580nm, and a green crystal that emits 490nm of light. Bicron Saint-Gobain Crystals & Detectors provided us the red crystal and Eljen Technology provided the green crystal. We note that the scintillators are, in fact, plastic and not a true crystal. Each scintillator is PMMA (polymethyl-metharylate) doped with an appropriate dye. Historically, these scintillators are referred to as crystals, and we have followed that practice.

Bicron supplied us with BC-430 red emitting polished bulk scintillator material. The bulk material is in a square shape with dimensions 5" x 5" x 10mm thick. We ordered them as a square slab so we could customize all the parts of the system. Therefore, we were able to play around with the crystal shape by ourselves so that the entire system

appropriately fitted together. We cut the crystal into the shape of a circular rod with 3mm diameter for the circular surface and the rod was 10mm long. The BC-430 crystal has a density of 1.032g/cc, which is very close to water. The density of a human body is very close to 1.0g/cc, so this is an advantage. We would like to have the density of the crystal to be as close to human density as possible, so we can be assured the crystal will have approximately the same reactions to the radiation as the human body.

Ideally, we want our crystal to have a large light output, and a short rise and decay time. But due to the properties of the red emitting crystal, no manufacturer can produce a crystal with a large light output. The rise time in this case is a fast 3.2 ns, but the decay time is a bit slower than ideal. If the decay time is too slow, then the crystal will still be giving off light before the next interactions occur. This will spoil the accuracy of response and prevent our integrator from subtracting away noise.

The green scintillator crystal we use is an EJ-260 green emitting plastic scintillator from Eljen Technology distributed by Apace Science. This crystal emits 490 nm wavelength of light. The light output of EJ-260 is 60%. Compared to BC-430 (red crystal), this will give us more light. Other specifications also look ideal; for example, the density of EJ-260 is 1.02 g/cc and the refractive index is 1.58. Both red and green crystals have similar properties.

The reason we chose these crystals from different manufacturers is because we were trying to find the best possible crystals. Bicron made the best red crystal. Their specifications meet our requirements and needs. Bicron also made green scintillator crystals, called BC-428, but the light output is too small, it only has a 36% light output compared to the Eljen EJ-260 with light output of 60% (percentage are referenced to anthracene).

We feel that we have found the best scintillators available. However, if other companies can provide a crystal with better properties than mentioned above, then there is no problem using crystals from those manufacturers. There are various kinds of optical fibers, the most important thing we need to consider is which fiber material

we want. There are two common broad classes of fibers, silica fibers and plastic fibers. Silica fiber is stiffer and stronger, whilst the plastic is more flexible and more fragile.

Optical Fiber

In medical practice we want something that can gives us flexibility of movement but is also strong enough that it does not break easily. We also want the fiber to be as small in diameter as possible. A small fiber diameter can provide convenience for inserting the fiber *in vivo*.

While the glass fiber is stronger and stiffer, it also transmits the light better than the plastic fiber. Plastic fibers has higher losses, especially for short wavelengths of light. However, the plastic fiber also has the advantage that it does not transmit ultraviolet light. This will help to attenuate the background signal from Cerenkov radiation. Plastic fibers also have a larger acceptance angle. So they will collect and transmit more of the light emitted from the scntillator crystal. All of these factors must be weighted against the increased losses of the plastic fiber.

In this experiment, we will use the plastic fiber. Mohammad Ali Alhabdan had already proved that the efficiency and ease of use between those two fibers are incomparable. Plastic fiber surely is much more suitable in our case and in the medical practice situation. The fiber is jacketed with black plastic to prevent any external light entering the fiber and being transmitted.

The fiber we are using is from Edmund Optics Singapore Pte. Ltd. called “Jacketed Optical Grade Light Guides” with stock number N02-536. This fiber has the diameter of 1000 microns - this includes the core and the clad. The outer diameter is 2.20 mm, including the core, clad and jacket. The core itself has the diameter of 980 microns. The core of the fiber is made of acrylic polymer PMMA (polymethyl-methacrylate) and the outer layer (clad) is made of fluorine polymer. The jacket is made of black polyethylene.

For light to transmit through the fiber, the core must have a higher refractive index than the clad. The core has the refractive index (n_1) of 1.492 and the clad has the refractive index (n_2) of 1.402.

Not all light coming from every angle can be transmitted through the fiber. There is an acceptance angle of 61°. Below is a diagram to illustrate the meaning of acceptance angle.

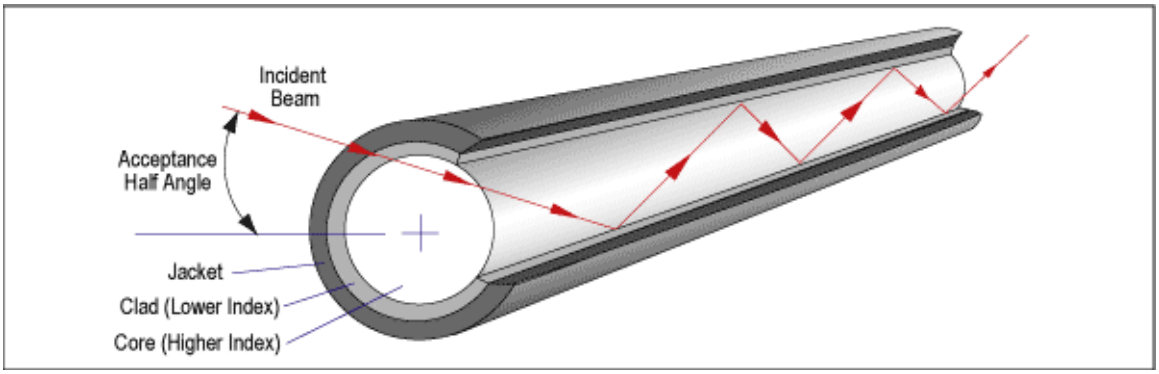

Fig 1: Structure of the optical fiber with acceptance angle.
(http://www.edmundoptics.com/onlinecatalog/DisplayProduct.cfm?productid=1352)

Any incoming light that has an angle greater than 61° can be totally transmitted. Normally, the bigger the acceptance angle, the better it is. As for the attenuation, this fiber has maximum attenuation of 0.21dB/m, which is acceptable. The attenuation should be as small as possible. The fiber doesn't respond the same to all ranges of wavelengths; it responds better to a certain range of wavelengths. We planned to use 490 nm and 580 nm of light in this experiment. The fiber responds well to both wavelengths.

Lenses

When the scintillator crystal emits light and the light is transmitted through the fiber to the distal end, we need to collect as much light as we possibly can. The way to achieve this is by placing two lenses at the distal end of the fiber. One lens will collect the light that is coming out from the fiber, and direct the light to parallel rays, the second lens will re-converge the parallel rays and focus them onto the window of the photodiode.

Below is a simple diagram to illustrate the lens system:

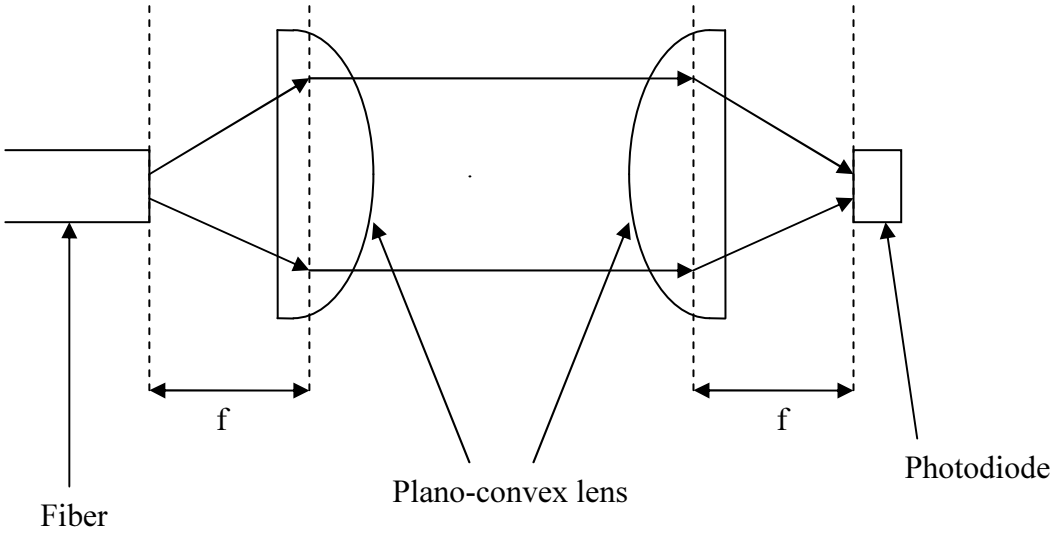

Fig 2: Two Plano convex lenses are placed between the end of the fiber and the photodiode. First lens will collect the light coming out from the fiber and make them parallel. The 2nd lens will re-focus the parallel light into the photodiode window. The distance "f" is the focal length of the lens, and this should be the same for both sides to avoid magnification on the spot size.

By doing some simple calculation we can work out exactly what dimension of lenses we need to capture all the light. The best possible lenses we can find are 6mm diameter with 6mm effective focal length (F number equals to 1), Plano-Convex Lenses from Edmund Optics Singapore Pte. Ltd. with VIS 0° coated, stock number N47-460. This lens will catch most of the light in our case, but it will miss about 3° to 4° of total incoming light. It is better to choose a small lens because it will be much easier to make the whole system smaller and tidier. We use 2 lenses in this system, both lenses are placed the same distance to the adjacent object (i.e. the fiber and photodiode).

Optical Filter

Noise or background signal will always exist in any electronic system. In addition to the background that comes from the electronics, we will have background light created from Cerenkov and fluorescence processes occurring in the optical fiber. For our system, the background signal (fluorescence and Cerenkov radiation) can be reduced by using an optical filter.

The optical filter is designed to allow only a small range of wavelengths to pass though it. The rest of the signals will be blocked out. So the optical filter we use in our system needs to fit the wavelength range of the scintillator crystals.

The optical filter we use is called a “Bandpass filter” from Newport Spectra-physics. We’ve chosen one with a 590nm center wavelength for the red scintillator and one with a 485nm center wavelength for the green scintillator. The part numbers are XM-590-A and XM-485-A respectively. There are 3 different sizes available. Because our lens diameter is 6mm, we need to choose our filter close to that dimension. The best choice we have is type A with a 12.7mm diameter and 7.6mm diameter for minimum active area.

The filter is placed between the 2 lenses, so all the parallel light coming from the first lens will be filtered by the filter, then re-focused to the photodiode by the second lens. Below is a diagram to illustrate it:

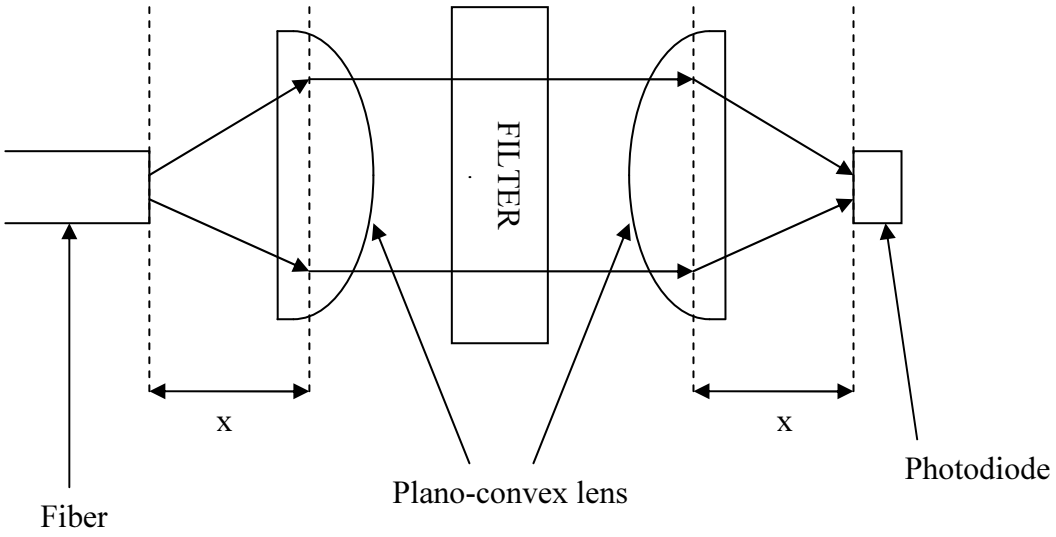

Fig 3: The optical filter is placed between the 2 Plano convex lenses. The parallel light from the first lens will all pass through the optical filter to filter out all the wavelengths that are outside the band width of the filter. The filter window size must be big enough to collect all the parallel light.

Photodiode

A photodiode is an electronic device that will convert a light signal into an electrical signal. In our experiment we need a photodiode that has a good response to the wavelengths we are working with. The photodiode we use in this experiment is BPW21 Photodiode from RS Electronics Components with RS stock number 303-719.

This photodiode has a small dimension in overall size. The detecting window is about 5.9mm diameter. Because this photodiode is placed after the second lens we need to focus all the light from the second lens into this detecting window. The response of this photodiode is better than the human eye. The peak spectral response of this photodiode is 560nm. Here is a diagram to show the spectral sensitivity of BPW21:

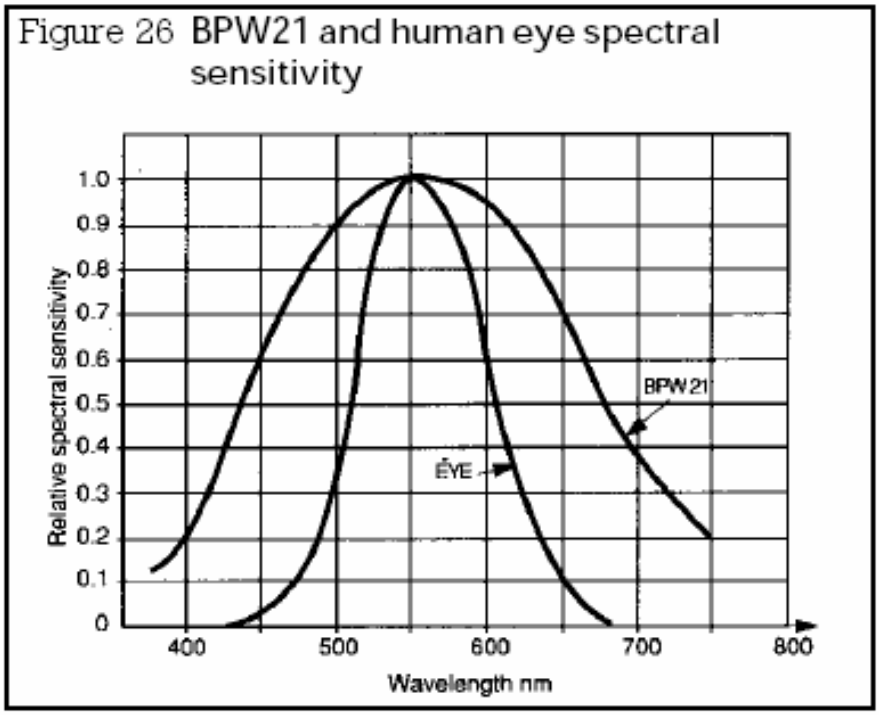

Fig 4: The photodiode BPW21 sensitivity V.S. wavelength in comparison to the human eye sensitivity (Diagram source from RS Data Sheet Photodiodes issued September 2002).

The wavelengths that we are working with are 580nm and 490nm. As you can see, they both sit on the points with reasonable sensitivity. The photodiode is mounted on an electronic circuit board. The signal is then amplified by op-amps. The signal will then be integrated by integrating the crystal signal plus the noise (electronic background) first, then by integrating the noise (electronic background) only.

The trigger pulse from the Linear Accelerator will be the timing. The result from each pulse after background subtraction will be added until the treatment stops. A liquid crystal display is placed to show the result.

The workshop of the Physics and Astronomy Department from University of Canterbury assembled all the parts together for us. The scintillator crystal was place in a seat that is attached to one end of the fiber. Both ends of the fiber should be polished smoothly to ensure best efficiency of light transmittance. A cap is placed to cover the crystal and also to hold it upright. The cap is strong enough to keep away any unnecessary force that might cause damage to the crystal.

When the crystal and the fiber are attached, special cement from Bicron should be used to hold both objects together. The cement is designed so that when crystal and fiber are attached to each other, the light will transmit straight through the cement without causing any interference, such as blocking the light or attenuation. The other end of the fiber is fitted into a bigger male cap with the first lens in it. The optical filter can be fitted inside the cap too, but it is not fixed; it can be removed. In our experiment we will measure the signal with filter and without filter, so it is preferable to make the filter removable.

There will be a female cap attached to one side of the electronic box, so that the fiber can slot into it and transmit the light into the photodiode. The female cap contains the second lens that will focus the incoming light to the photodiode which is closely placed behind the lens. The female and male caps are fitted to ensure a light tight environment. This is very important in this experiment, as any light entering or escaping from the system will affect the results.

Last is the electronics that takes over the processing step with the amplifier and integration process. Below is the detailed drawing of the whole system:

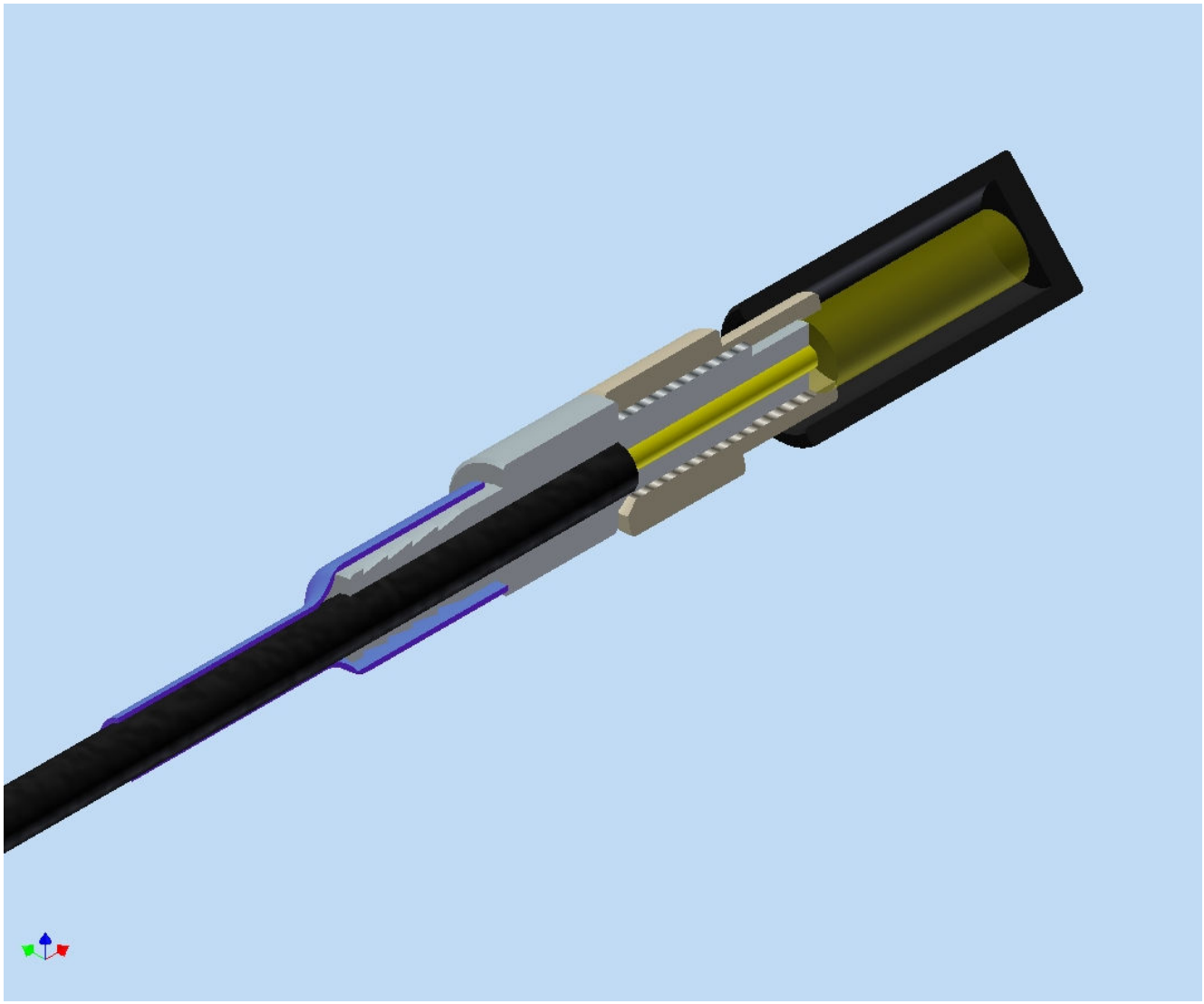

Fig 5: This is the end where the scintillator crystal is located. The yellow cylindrical object is the crystal. It is attached to the fiber and protected with a casing. There are various parts of plastic and metal to secure the attachment between the fiber and the crystal.

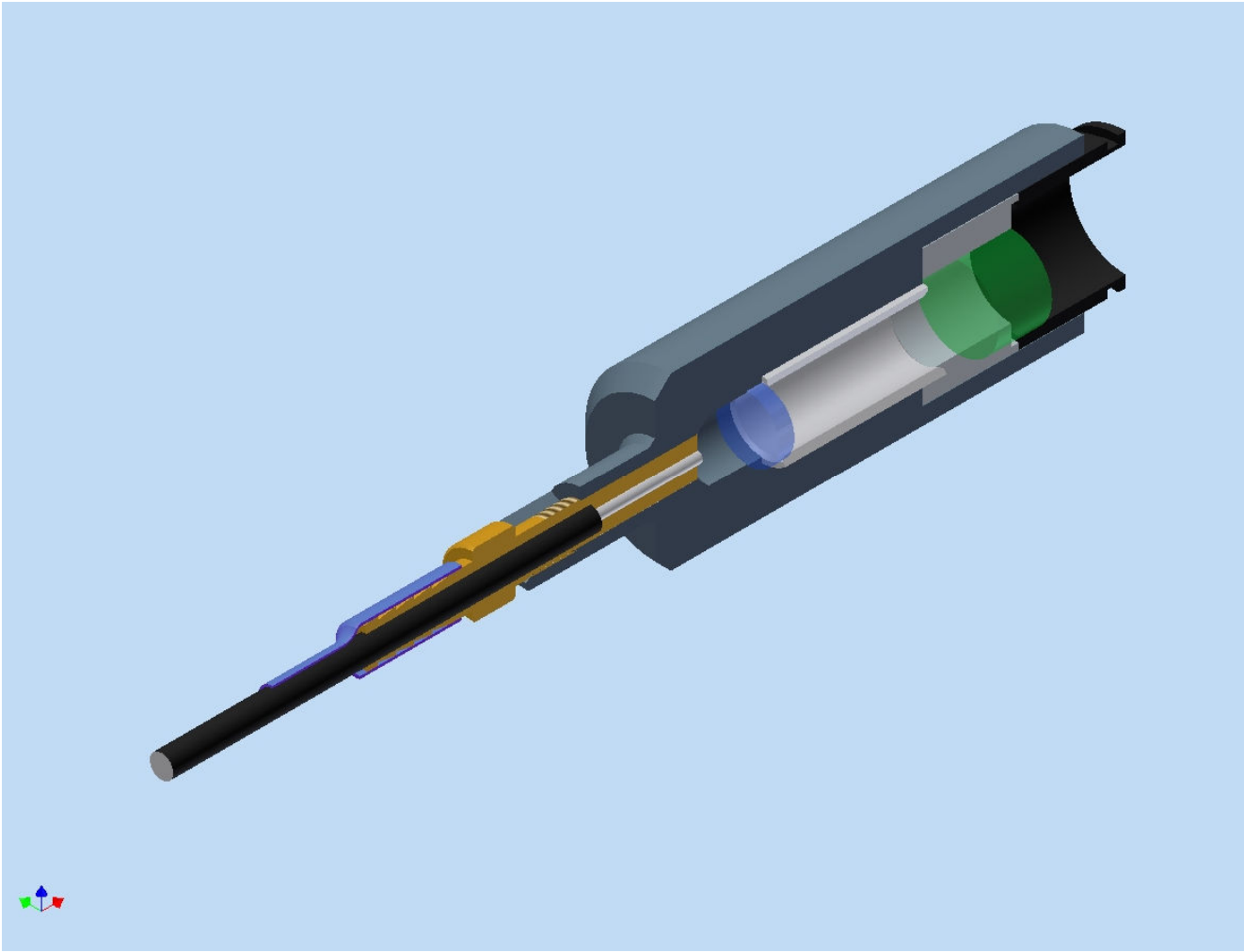

Fig 6: This is the distal end of the fiber. The blue disc is the first Plano-Convex lens, followed by a green cylindrical block which is the optical filter. When light is coming out from the fiber, the lens collects the light and converts it to parallel rays which then pass through the filter to filter out the background signal. This housing is attached to the fiber.

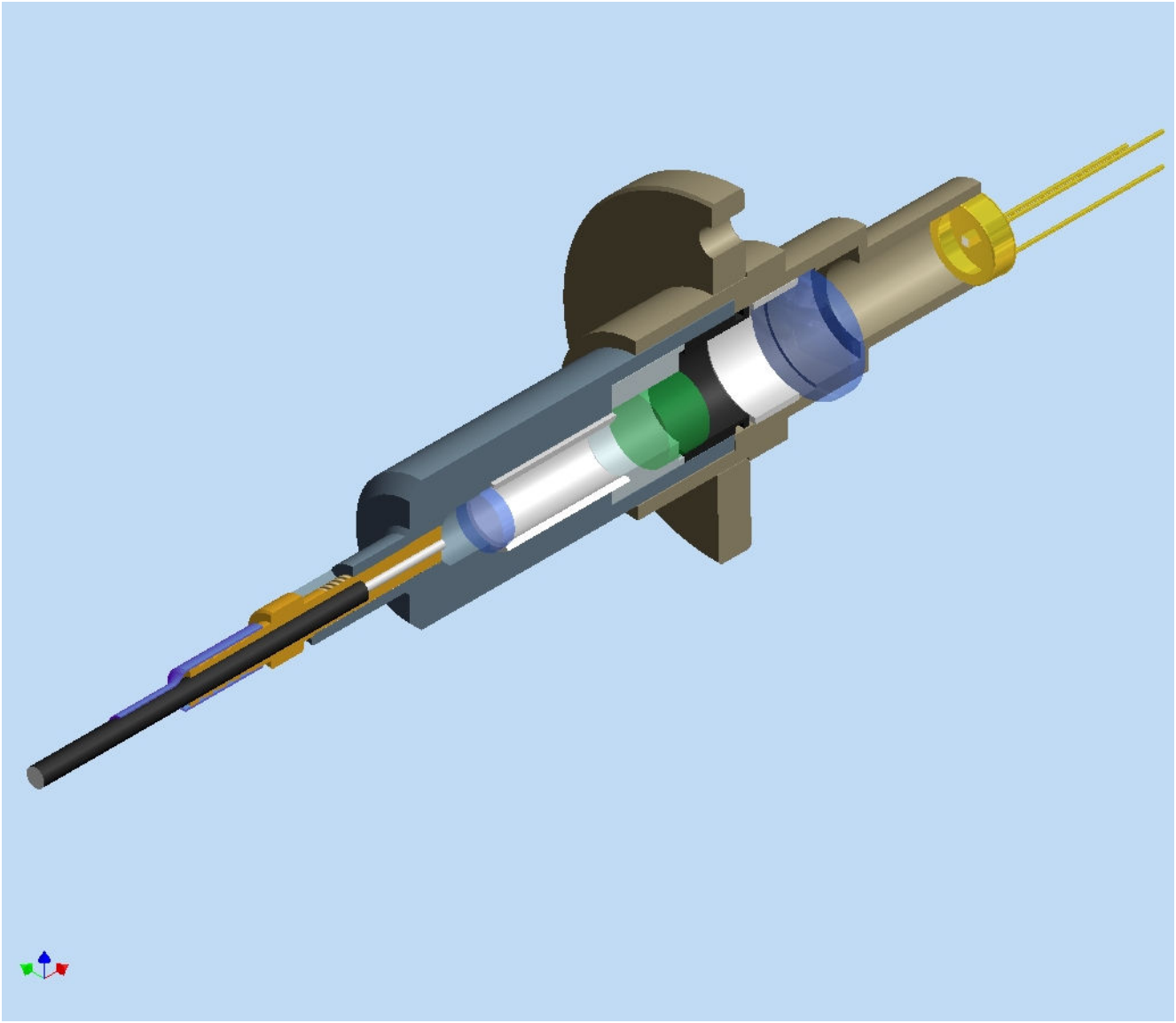

Fig 7: This is the view when the fiber is plugged into the electronic box. The dark brown housing which contains the 2nd Plano –convex lens and the Photodiode (the gold object with 3 wires) is placed in the electronic box. When we slot the fiber housing (Fig 6) into the dark brown housing, we have the complete system. The light passing through the filter will be collected by the 2nd lens and focused into the photodiode active window. The signal is then passed to the integrator for processing.

METHODS

Part 1

To compare the red scintillator crystal to the green crystal, we need to find out the SOBR (Signal to Optical Background Ratio). We do this in this situation when the beam is perpendicular to the scintillator crystal. Here we define the SOBR to be the response of total signal (crystal and fiber) divided by the background (fiber) signal. We note this is a bit different from the traditional definition of SNR (signal to noise ratio). However, for this work the definition given above is the important quantity. It gives us a ratio of the signal we get against the background. What we need to do is irradiate the fiber and scintillator crystal and record the reading, then do the same thing again but with only the fiber. We then divide the readings to get SOBR.

First we need to place the crystal at the iso-center of the machine. We can do this by using the lasers in the room which can give us an accurate point for the iso-center. Below the crystal, we've placed two blocks 4cm thick of solid water - this gives us a total of 8cm thick of solid water below the crystal. The reason we have these solid water blocks is to prevent any back scatter from the surrounding environment. On the top of the crystal, we've placed two blocks of solid water - they are 1.0cm and 0.5cm thick. This adds up to 1.5cm of thickness which is the D_{max} of the 6MV machine. This will place the crystal in the plane of a maximum dose.

We expose the system to the following sequences of Monitoring Units (MU):
1, 2, 4, 8, 16, 32, 64, 128, 256, 512, 1024.

The MU is doubled each time. The reason for this is we want to see if the system is linear. The readings from the LED of the electronic box represent the response of the system to the radiation. Because the MUs are doubled each time the response we going to have should be doubled as well.

We set the field size to a half field of 20x20 cm^2. Place the crystal at iso-center and leave the rest of the fiber exposed to the beam. There is about 9cm of fiber getting irradiated.

We extend another 1cm of the field out so that the whole crystal is irradiated even when the crystal is placed at iso-center. This is to ensure the center of the crystal is placed at the iso-center, not the tip of the crystal. Here is a diagram to show the situation:

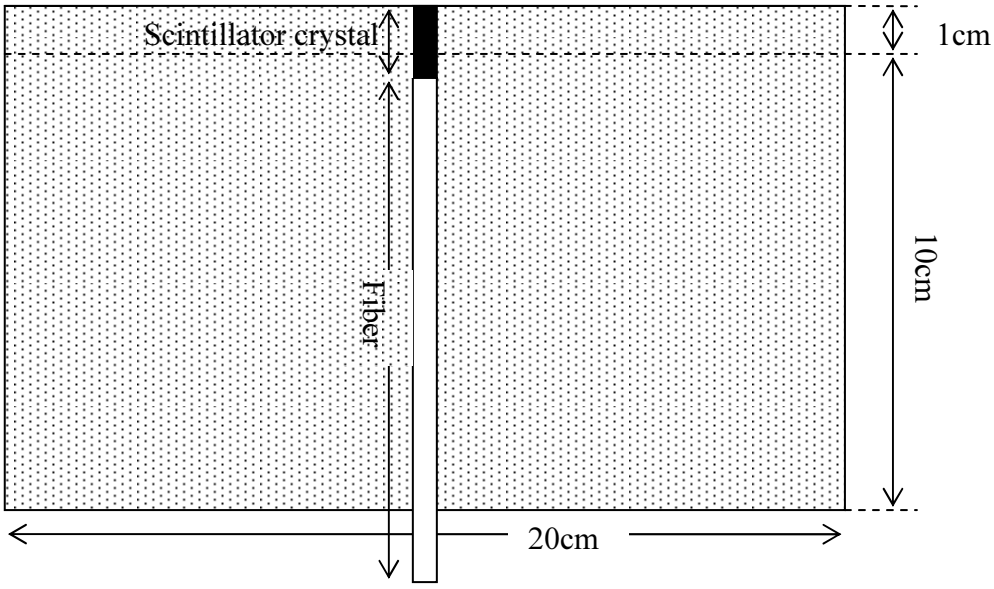

Fig 8: Experiment set up for Part 1. The center of the crystal is placed at iso-center. The field size is a 20x20cm^2 half field. An extra centimeter of "Y2" is extended. Y2 is the name given for the top jaw of the LINAC.

After we recorded the readings for all different monitoring units, we repeated the experiment, but this time we irradiated the fiber only. At this moment, we bring the extended 1cm of field back, so now we have the proper 20x20cm^2 half field. The reason for this is to try to make the signal from the fiber close to each other at both situations. In both situations, we take the readings at least twice, then take the average - this will give us a better result. If the two measurements do not agree, we repeat both situations 3 times or more.

After all the readings are recorded for both crystals, we should have the average values for each MU from the "Fiber" signals and "Crystal + Fiber" signals. We used Microsoft Excel to plot a graph and state the slope of both line of fits, and divided them from each other to give us the SOBR.

Method - Part 2

The second stage of the experiment is to change the field shape to the outline of the system. So we set the field like the diagram below:

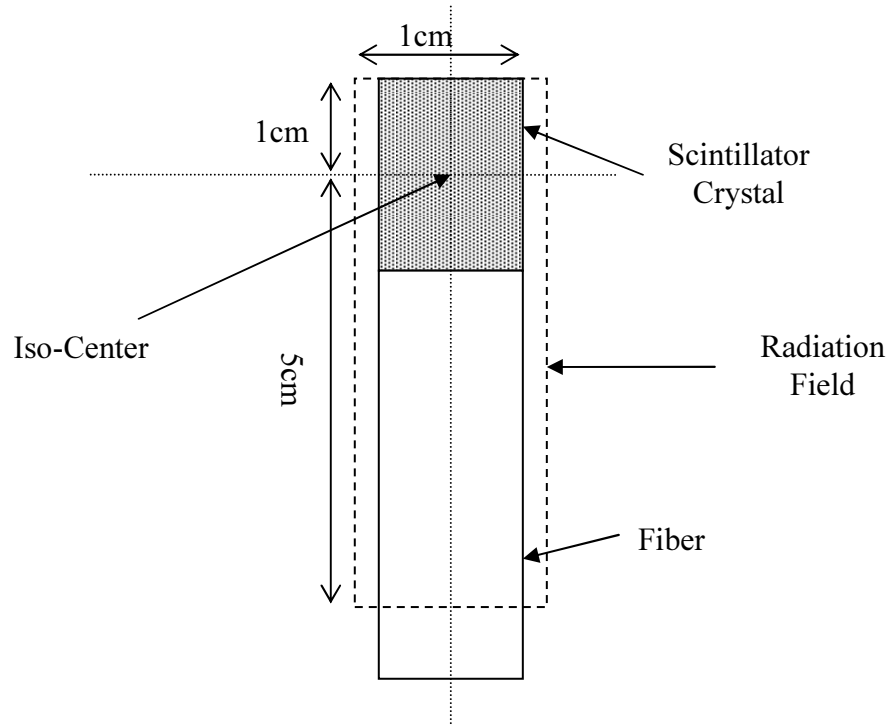

Fig 9: Experiment set up for Part 2. The field is adjusted to the dimensions that are closely matched to the outline of the system. The width is 0.5cm from iso-center for both sides. Total length is 6cm. Iso-center is aiming at the center of the crystal.

We use the same monitoring unit sequence to record the response of our detector. Finally we plot the results to see if the slopes of the line compares with the results from the 20x20 cm^2 half field. This will tell us which field shape setting gives us a better result.

Method – Part 3-1

The last stage of the experiment is divided into two parts. In both parts the beam is rotated to various angles. In all the previous stages of the experiment, the beam has been perpendicular to the scintillator crystal. The reason we want to test with different beam angles is because we want to test how our detector responds to Cerenkov radiation.

We will rotate the beam angle in segments of 5°, starting from 0° then 5°, 10° and so on, until we reach 45°. We do the same for the other side. A fixed MU of 200MU is used in this part. The field is a $10x10cm^2$ full field.

Below is a diagram to illustrate the set up.

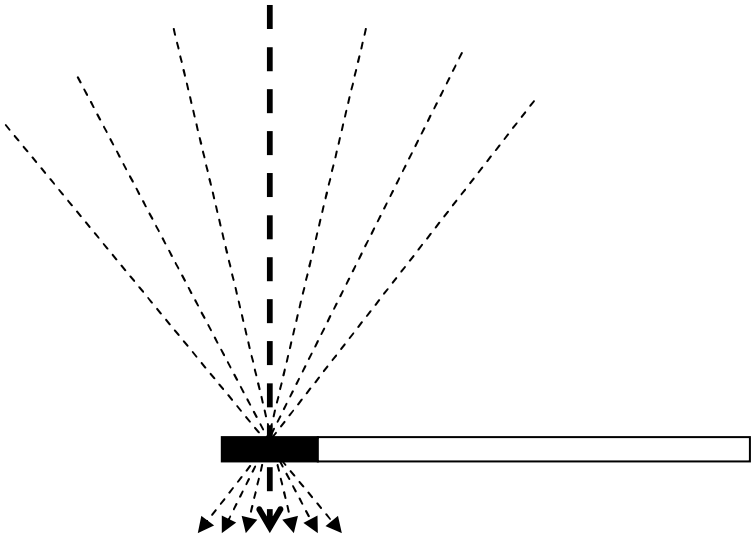

Fig 10: The system is placed laterally to the radiation beam. The iso-center is at the center of the scintillator crystal. The beam angle is changed from -45° (315°) to 45° in segments of 5°. The field size is a $10x10cm^2$ full field.

The beam is rotated to both left and right once it has reached 45°. We irradiate the fiber only first, and then repeat the procedure with the scintillator crystal plus the fiber. Lastly, we work out the SOBR and the response.

The system is placed into an open ended plastic square rod. The rod is held by a metal clamp, which is placed outside the beam field. This is very important because the metal clamp should not be in the way of the field - this would create excessive scatter. One end of the square rod will be located close to the iso-center. The scintillator crystal will exit from the end that is close to the iso-center and be placed right at the iso-center. The rest of the fiber will come out from the other end and extend to the photodiode.

Because the density of the plastic rod is small and we are dealing with a 6MV energy beam, we can ignore the small effect the plastic square rod will cause. The surroundings of the crystal should be as clear as possible, so the back scatter is identical no matter where the beam is coming from. We were especially careful to watch out for any metal objects like trolleys.

Using 200MU for each angle, we take the reading 2 times and average them. When we irradiate only the fiber, the set up will be a little different. We place the fiber into the plastic rod and irradiate both the plastic rod and the fiber. This is because we want the fiber to be placed nice and flat to get repeatable results. Below are 2 diagrams showing the set up of the scintillator crystal and the fiber.

Irradiate the Scintillator Crystal

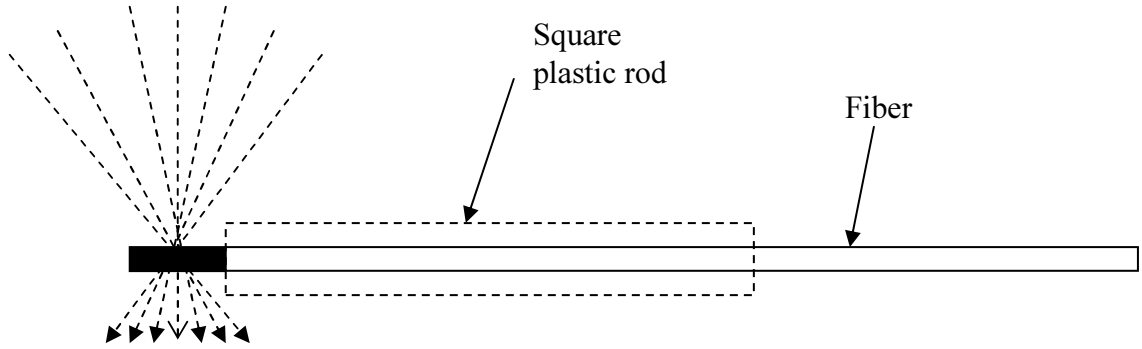

Fig 11: The system is placed inside a low density plastic square rod with only the scintillator crystal exiting from one end. The plastic rod is there to support the system so the system is horizontally in mid-air. This gives us a more consistent result.

Irradiate the fiber

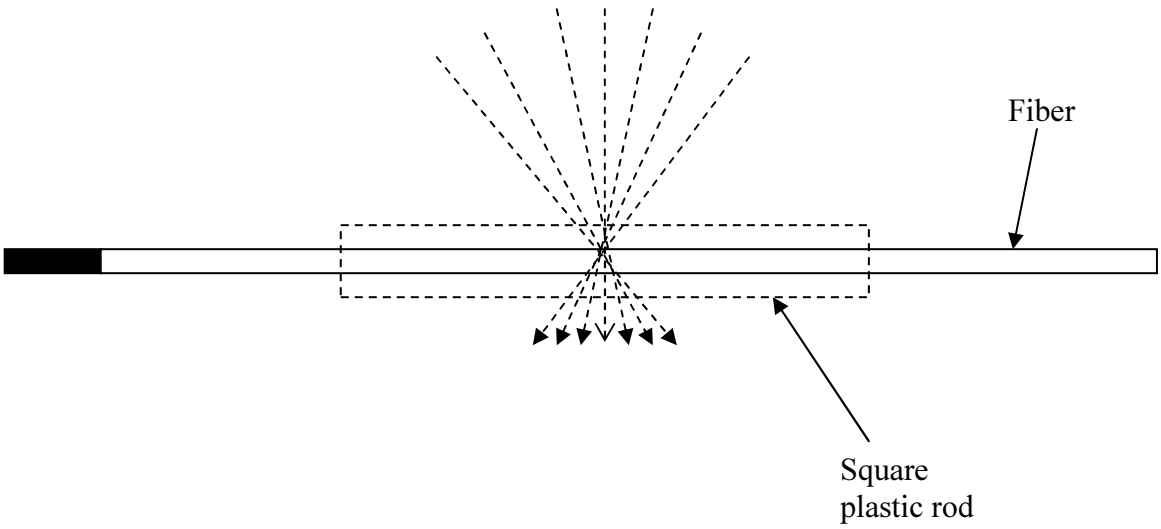

Fig 12: When irradiating the fiber, we slide the plastic rod further down so the crystal is out of the way from the beam field. This is to make the fiber straight and horizontal. We place the center of the rod at iso-center. When the beam angle is changed, the fiber is flat and straight on both sides of the iso-center.

When irradiating only the fiber, the crystal should be placed as far away from the beam field as possible. The beam should be placed near the center of the rod, so that it has plenty of uniform space on both sides. The metal clamp needs to be away from the beam field. Before starting the measurements, we rotate the gantry to both sides and make sure it does not collide with any of the equipment. The set up uses no solid water in this case. The system is free in mid-air. All measurements are made at least twice and averaged.

Method – Part 3-2

The 2nd part of the experiment is to rotate the scintillator crystal 90°, which is pointing our detector at the LINAC, and then to fire the beams from different angles just like method 3.1. The range of angles we are using this time are from 90° to -90° (or 270° according to the gantry reading). We will use the same square plastic rod and the metal clamp, with the detector crystal exiting out from one end and located at the beam iso-center. We use 200MU for each angle twice and take the reading and average it.

Here is a simple diagram to illustrate the set up:

Looking from side (Not in Scale)

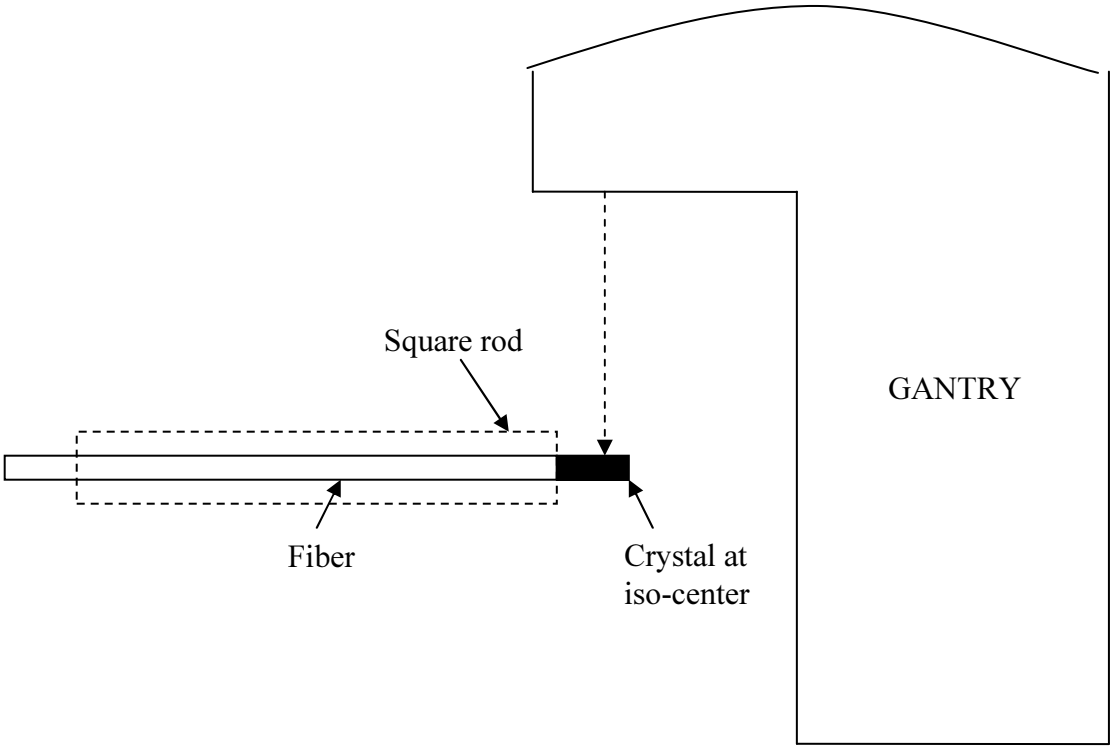

Fig 13: The system is rotated, the crystal is now pointing at the gantry. The center of the crystal is placed at iso-center. The system is placed inside the plastic rod and only the crystal is exiting from one end.

The purpose of this part of the experiment is to investigate how the detector responds to different angles of incoming radiation. We expect there to be no angular dependence in this geometry. However, an angular variation would indicate irregularities in the detector, like a partial glue bond between the scintillator and the fiber. Again, when doing this part of the experiment, we make sure both sides of the LINAC are clear and make sure when the gantry is rotated to 90° and 270° that it does not collide with anything.

Dark Counts

Dark counts are the readings that appear on the liquid crystal display of the integrator when the machine is "beam on" but the detector and fiber is not actually in the beam field. In another words, these are the signals registered by the electronics that are not subtracted by the integrator. We need to find the dark counts first. In this research, we will use 1, 2, 4, 8, 16, 32, 64, 128, 256, 512 and 1024 MU with a $20x20cm^2$ field. Both red and green systems will need to be tested. We place the red system into the LINAC room with Channel 1 connected. The green system is connected to Channel 2 but placed right next to the electronic box (containing the integrator which gives us the response of the detector) which is placed in the control room. The red system is not in the field of the beam.

The LINAC is switched on with the above MU and field size, and the response is recorded for the red scintillator. The same procedure is then repeated but with the green system in Channel 1 and placed inside the LINAC room, and the red system in Channel 2 and placed beside the electronic box in the control room. We take 3 readings for the green scintillator for each MU and average the readings. These readings are registered as the dark counts for Methods Part 1 and 2.

The second part is to set the field size to $10x10cm^2$ with MU equal to 200. We then do the same for both red and green systems as we did previously. The results are the dark counts for Methods Part 3.

After we've obtained all the dark counts for every part of this research, we will apply them to every subsequent measurement. In every experiment, we have taken the average of all the readings. Then we take the average readings and subtract the dark counts.

RESULTS – DARK COUNTS

Table 1: These are the dark counts of the red system for Methods Part 1 and Part 2. Each MU is tested 3 times then the average is calculated.

DARK COUNTS TEST FOR RED SYSTEM				
MU	ROUND 1	ROUND 2	ROUND 3	AVERAGE
1	14	10	6	10
2	20	25	11	18.666667
4	43	40	41	41.333333
8	99	89	117	101.66667
16	192	177	165	178
32	382	383	398	387.66667
64	821	813	759	797.66667
128	1497	1482	1621	1533.3333
256	3103	2973	3102	3059.3333
512	6238	6083	6175	6165.3333
1024	12371	12278	12238	12295.667

Table2: These are the dark counts of the green system for Methods Part 1 and Par 2. Each MU is tested 3 times then the average is calculated.

DARK COUNTS TEST FOR GREEN SYSTEM				
MU	ROUND 1	ROUND 2	ROUND 3	AVERAGE
1	18	12	9	13
2	18	21	24	21
4	46	39	53	46
8	103	89	101	97.66666667
16	163	189	201	184.3333333
32	355	404	392	383.6666667
64	744	816	783	781
128	1582	1627	1688	1632.333333
256	3245	3042	3211	3166
512	6359	6371	6174	6301.333333
1024	12659	12646	12792	12699

Table 3: This is the table showing the dark counts for both red and green systems. These dark counts are for Methods Part 3. The average dark counts for both systems are very close to each other.

DARK COUNTS FOR GREEN SYSTEM				
MU	ROUND 1	ROUND 2	ROUND 3	AVERAGE
200	2536	2551	2525	2537.3333

DARK COUNTS FOR RED SYSTEM				
MU	ROUND 1	ROUND 2	ROUND 3	AVERAGE
200	2475	2390	2534	2466.3333

RESULTS – PART 1

Table 4: This is the result for Part 1. Each fiber-only signal and crystal signal reading was taken twice; average value is then calculated. The column AVG-BC stands for "Average value minus dark counts". The set up of this experiment is using the red system in channel 1, NO filter was used, the field size is 20x20cm^2 half field. The SOBR is calculated by using the slopes of the plots.

CHAN 1 RED SYSTEM WITH **NO FILTER**, 20X20 HALF FIELD								
MU	FIBER	FIBER	AVERAGE	AVG-BC	RED	RED	AVERAGE	AVG-BC
1	25	36	30.5	20.5	267	260	263.5	253.5
2	62	53	57.5	38.833333	505	489	497	478.3333333
4	105	105	105	63.666667	1017	1040	1028.5	987.1666667
8	224	224	224	122.33333	2024	1992	2008	1906.333333
16	421	450	435.5	257.5	3988	4035	4011.5	3833.5
32	768	862	815	427.33333	8059	8129	8094	7706.333333
64	1752	1618	1685	887.33333	16150	16216	16183	15385.33333
128	3420	3206	3313	1779.6667	32102	32134	32118	30584.66667
256	6780	6907	6843.5	3784.1667	64811	64543	64677	61617.66667
512	13449	13607	13528	7362.6667	129257	129042	129149.5	122984.1667
1024	27049	27221	27135	14839.333	258375	257434	257904.5	245608.8333
							SOBR	16.57685665

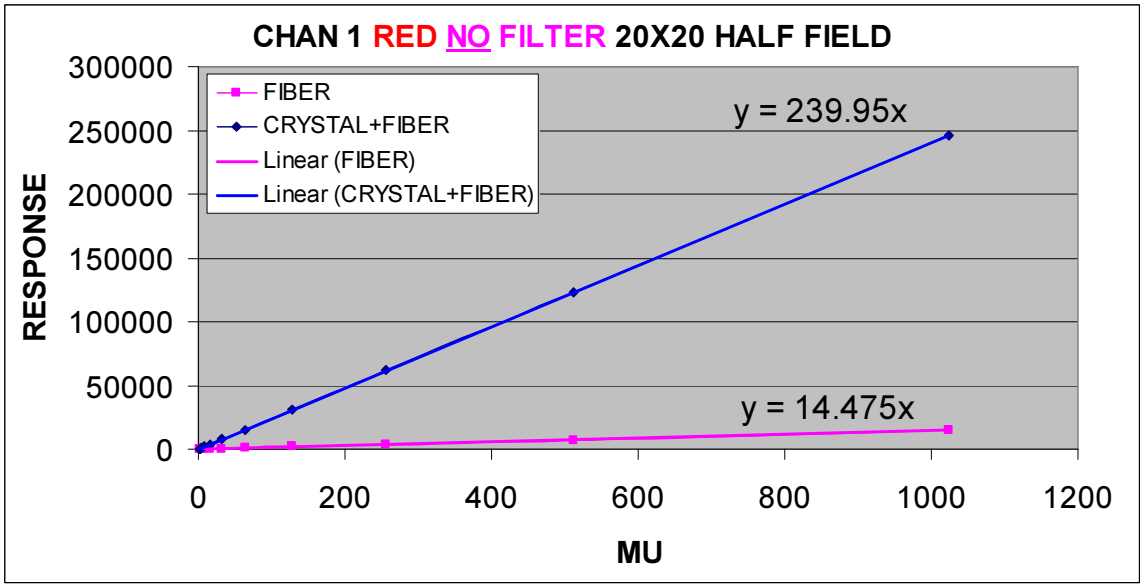

Fig 14: Plot Result of Part 1 for RED system with NO filter. Field size is 20x20cm^2 half field. Slope for fiber and main signal are 14.475 and 239.95 respectively. SOBR is 16.58

Table 5: Result of Part 1. Red system is used WITH filter. The field size is 20x20cm^2 half field.

CHAN 1 RED SYSTEM **WITH FILTER** 20X20 HALF FIELD								
MU	FIBER	FIBER	AVERAGE	AVG-BC	RED	RED	AVERAGE	AVG-BC
1	16	18	17	7	15	34	24.5	14.5
2	32	31	31.5	12.833333	27	37	32	13.33333333
4	58	46	52	10.666667	70	69	69.5	28.16666667
8	88	122	105	3.3333333	170	148	159	57.33333333
16	198	175	186.5	8.5	355	342	348.5	170.5
32	406	423	414.5	26.833333	619	736	677.5	289.8333333
64	799	854	826.5	28.833333	1305	1279	1292	494.3333333
128	1693	1666	1679.5	146.16667	2611	2565	2588	1054.666667
256	3292	3244	3268	208.66667	5190	5175	5182.5	2123.166667
512	6600	6522	6561	395.66667	10545	10372	10458.5	4293.166667
1024	13016	13080	13048	752.33333	20775	20689	20732	8436.333333
							SOBR	11.03001601

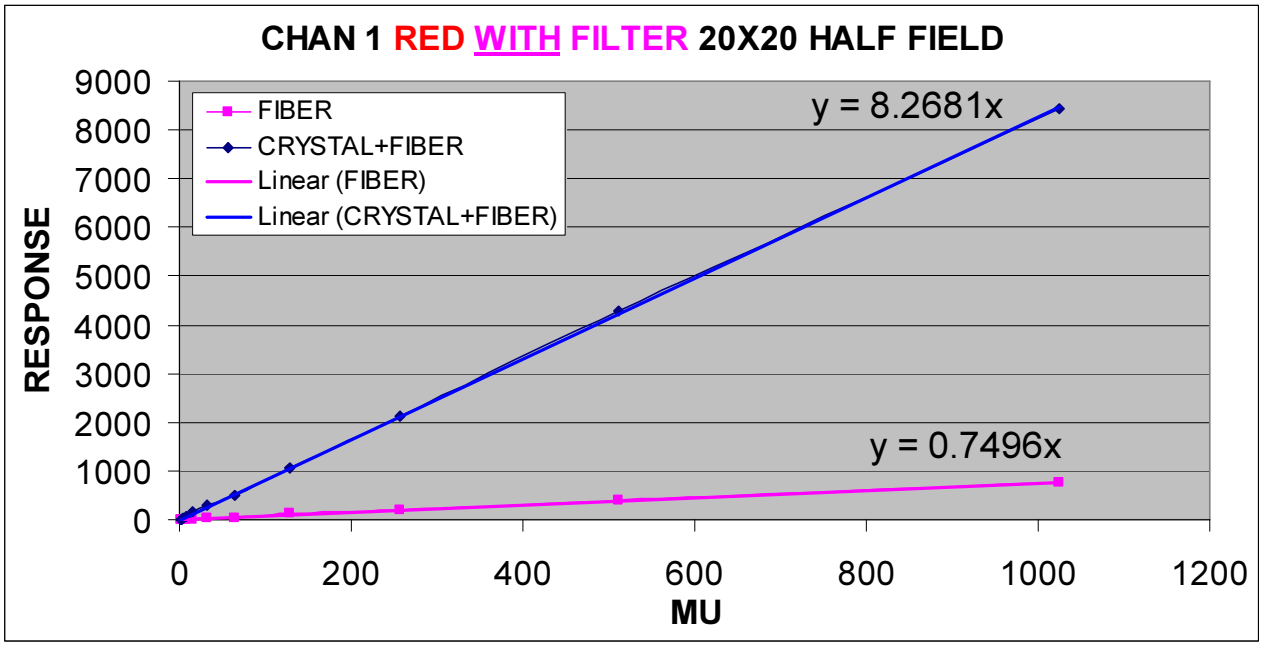

Fig 15: Plot Result of Part 1 for red system WITH filter. Field size is 20x20cm^2 half field. Slope for fiber and main signal are 0.7496 and 8.2681 respectively. SOBR is 11.03

Table 6: Result of Part 1 for green system with NO filter. Field size is 20x20cm^2 half field.

CHAN 1 GREEN SYSTEM WITH **NO FILTER** 20X20 HALF FIELD								
MU	FIBER	FIBER	AVERAGE	AVG-BC	GREEN	GREEN	AVERAGE	AVG-BC
1	38	32	35	22	307	339	323	310
2	59	64	61.5	40.5	619	646	632.5	611.5
4	118	112	115	69	1212	1274	1243	1197
8	224	226	225	127.33333	2462	2392	2427	2329.333333
16	456	413	434.5	250.16667	4806	4857	4831.5	4647.166667
32	973	794	883.5	499.83333	9808	9664	9736	9352.333333
64	1895	1813	1854	1073	19292	19566	19429	18648
128	3706	3623	3664.5	2032.1667	39043	38895	38969	37336.66667
256	7214	7291	7252.5	4086.5	77591	78079	77835	74669
512	14798	14905	14851.5	8550.1667	155792	155306	155549	149247.6667
1024	29772	29180	29476	16777	310982	310608	310795	298096
							SOBR	17.7378487

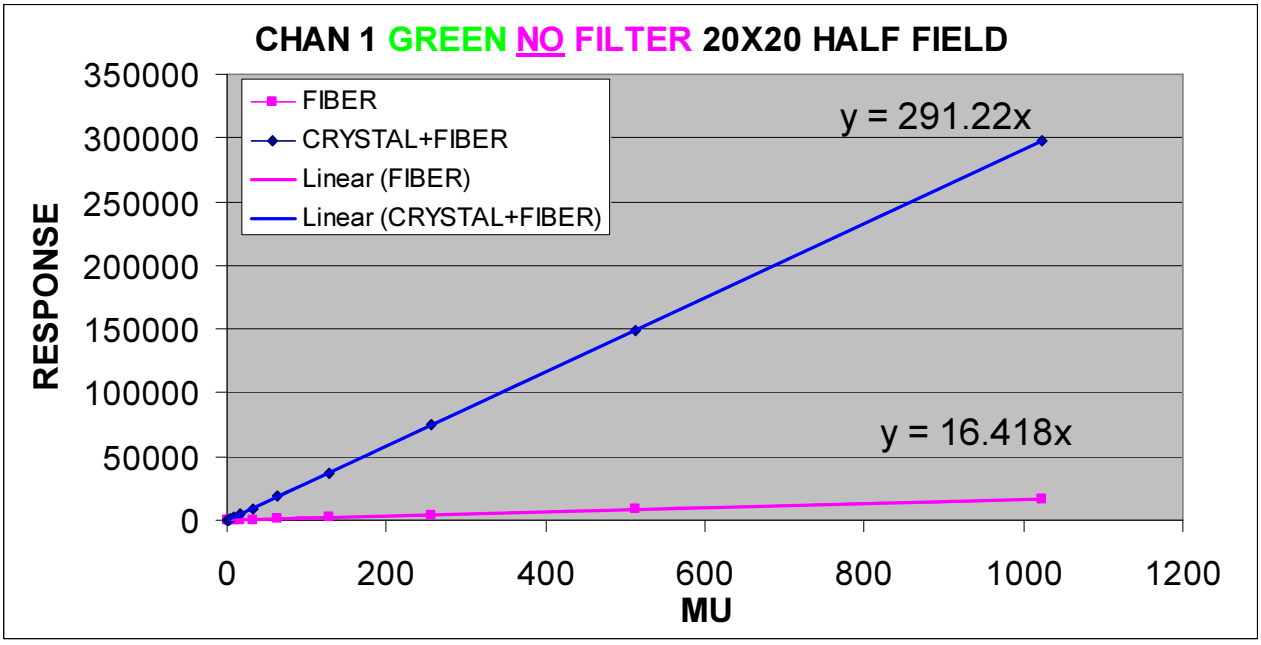

Fig 16: Plot Result of Part 1 for green system with NO filter. Field size is 20x20cm^2 half field. Slope for fiber and main signal are 16.418 and 291.22

Table 7: Result of Part 1 for green system WITH filter. Field size is 20x20cm^2 half field.

CHAN 1 GREEN SYSTEM **WITH FILTER** 20X20 HALF FIELD								
MU	FIBER	FIBER	AVERAGE	AVG-BC	GREEN	GREEN	AVERAGE	AVG-BC
1	12	24	18	5	48	42	45	32
2	25	33	29	8	110	110	110	89
4	49	58	53.5	7.5	207	217	212	166
8	119	104	111.5	13.833333	399	407	403	305.3333333
16	202	208	205	20.666667	832	844	838	653.6666667
32	408	428	418	34.333333	1712	1601	1656.5	1272.833333
64	766	896	831	50	3181	3221	3201	2420
128	1679	1670	1674.5	42.166667	6701	6515	6608	4975.666667
256	3150	3339	3244.5	78.5	13155	13053	13104	9938
512	6583	6725	6654	352.66667	26017	26231	26124	19822.66667
1024	13175	13412	13293.5	594.5	53106	52656	52881	40182
							SOBR	66.72466735

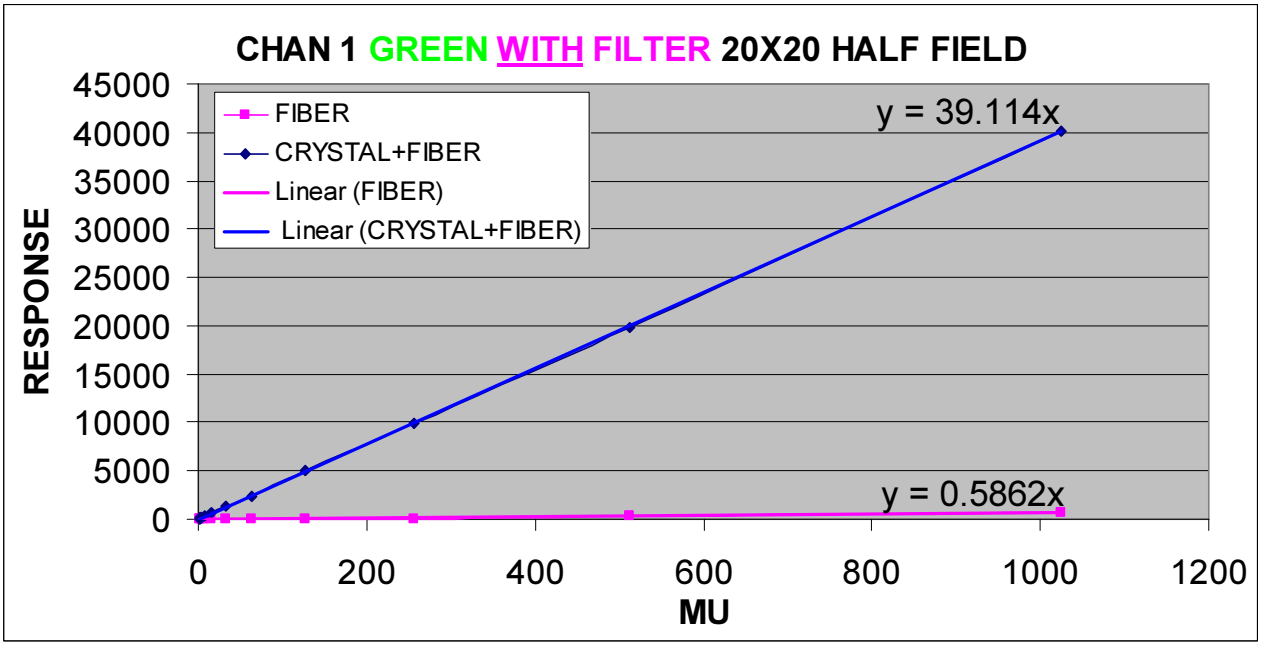

Fig 17: Plot Result of Part 1 for green system WITH filter. Field size is 20x20cm^2 half field. Slope for fiber and main signal are 0.5862 and 39.114 respectively. SOBR is 66.72

RESULTS – PART 2

Table 8: Result of Part 2 for red system with NO filter. Field size is X=1cm, Y1=5cm, Y2=1cm.

CHAN 1 RED SYSTEM WITH **NO FILTER** FIELD SHAPE SAME AS SYSTEM								
MU	FIBER	FIBER	AVERAGE	AVG-BC	RED	RED	AVERAGE	AVG-BC
1	12	14	13	3	195	217	206	196
2	34	33	33.5	14.833333	359	377	368	349.3333333
4	63	77	70	28.666667	783	738	760.5	719.1666667
8	123	122	122.5	20.833333	1592	1598	1595	1493.333333
16	299	243	271	93	3096	3079	3087.5	2909.5
32	513	495	504	116.33333	6172	6221	6196.5	5808.833333
64	1086	1036	1061	263.33333	12398	12491	12444.5	11646.83333
128	2133	2031	2082	548.66667	24865	24880	24872.5	23339.16667
256	4064	4273	4168.5	1109.1667	49554	49510	49532	46472.66667
512	8309	8288	8298.5	2133.1667	99650	99211	99430.5	93265.16667
1024	16488	16447	16467.5	4171.8333	198938	199541	199239.5	186943.8333
							SOBR	44.42902024

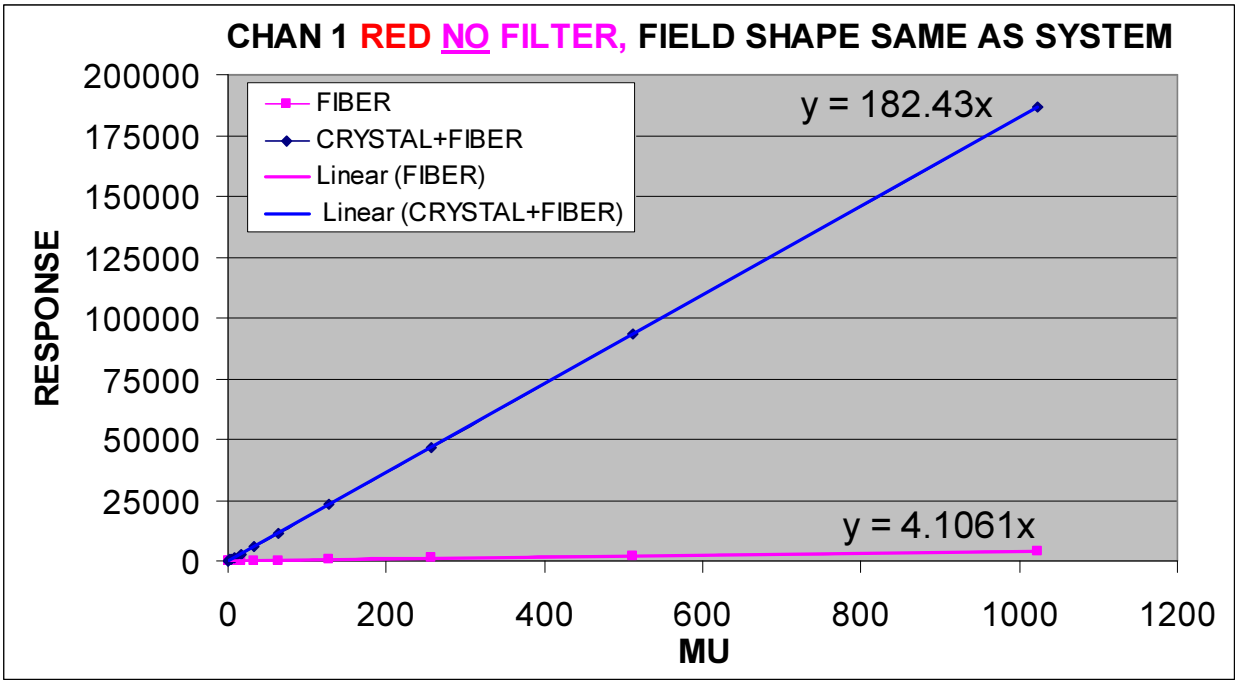

Fig 18: Plot Result of Part 2 for red system with NO filter. Field size is X=1cm, Y1=5cm, Y2=1cm. Slope for fiber and main signal are 4.1061 and 182.43 respectively. SOBR is 44.43

Table 9: Result of Part 2 for red system WITH filter. Field size is X=1cm, Y1=5cm, Y2=1cm.

CHAN 1 RED SYSTEM **WITH FILTER** FIELD SHAPE SAME AS SYSTEM								
MU	FIBER	FIBER	AVERAGE	AVG-BC	RED	RED	AVERAGE	AVG-BC
1	10	18	14	4	17	11	14	4
2	25	13	19	0.3333333	33	42	37.5	18.83333333
4	48	67	57.5	16.166667	78	56	67	25.66666667
8	106	107	106.5	4.8333333	156	181	168.5	66.83333333
16	180	183	181.5	3.5	301	325	313	135
32	414	407	410.5	22.833333	592	612	602	214.3333333
64	825	779	802	4.3333333	1181	1205	1193	395.3333333
128	1579	1566	1572.5	39.166667	2573	2438	2505.5	972.1666667
256	3195	3123	3159	99.666667	4875	4959	4917	1857.666667
512	6312	6445	6378.5	213.16667	9860	9795	9827.5	3662.166667
1024	12777	12737	12757	461.33333	19339	19057	19198	6902.333333
							SOBR	15.61947104

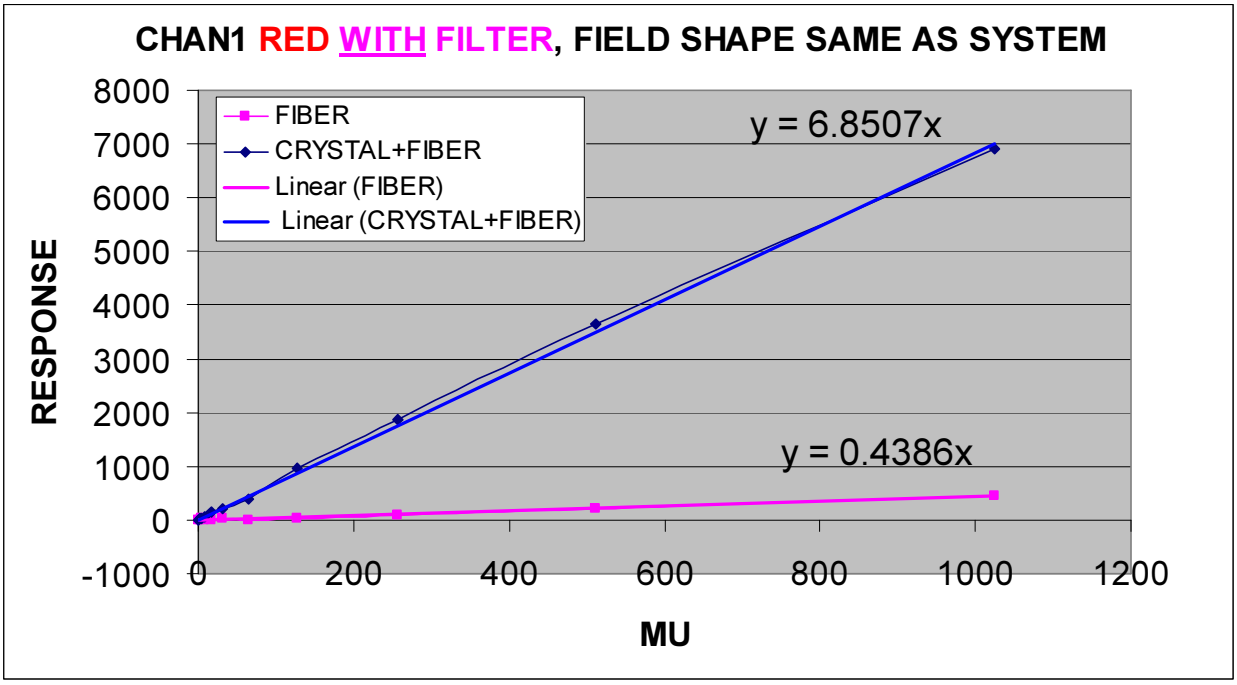

Fig 19: Plot Result of Part 2 for red system WITH filter. Field size is X=1cm, Y1=5cm, Y2=1cm. Slope for fiber and main signal are 0.4386 and 6.8507 respectively. SOBR is 15.62

Table 10: Result of Part 2 for green system with NO filter. Field size is X=1cm, Y1=5cm, Y2=1cm.

CHAN 1 GREEN SYSTEM **NO FILTER** FIELD SHAPE SAME AS SYSTEM								
MU	FIBER	FIBER	AVERAGE	AVG-BC	GREEN	GREEN	AVERAGE	AVG-BC
1	22	16	19	6	247	258	252.5	239.5
2	18	26	22	1	443	460	451.5	430.5
4	60	64	62	16	888	920	904	858
8	136	172	154	56.333333	1730	1892	1811	1713.333333
16	289	263	276	91.666667	3592	3673	3632.5	3448.166667
32	532	500	516	132.33333	7104	7229	7166.5	6782.833333
64	1093	1071	1082	301	13917	14717	14317	13536
128	2332	2330	2331	698.66667	27737	29525	28631	26998.66667
256	4388	4380	4384	1218	56062	58120	57091	53925
512	8781	8676	8728.5	2427.1667	114344	115938	115141	108839.6667
1024	17749	17438	17593.5	4894.5	233990	239986	236988	224289
							SOBR	45.47280755

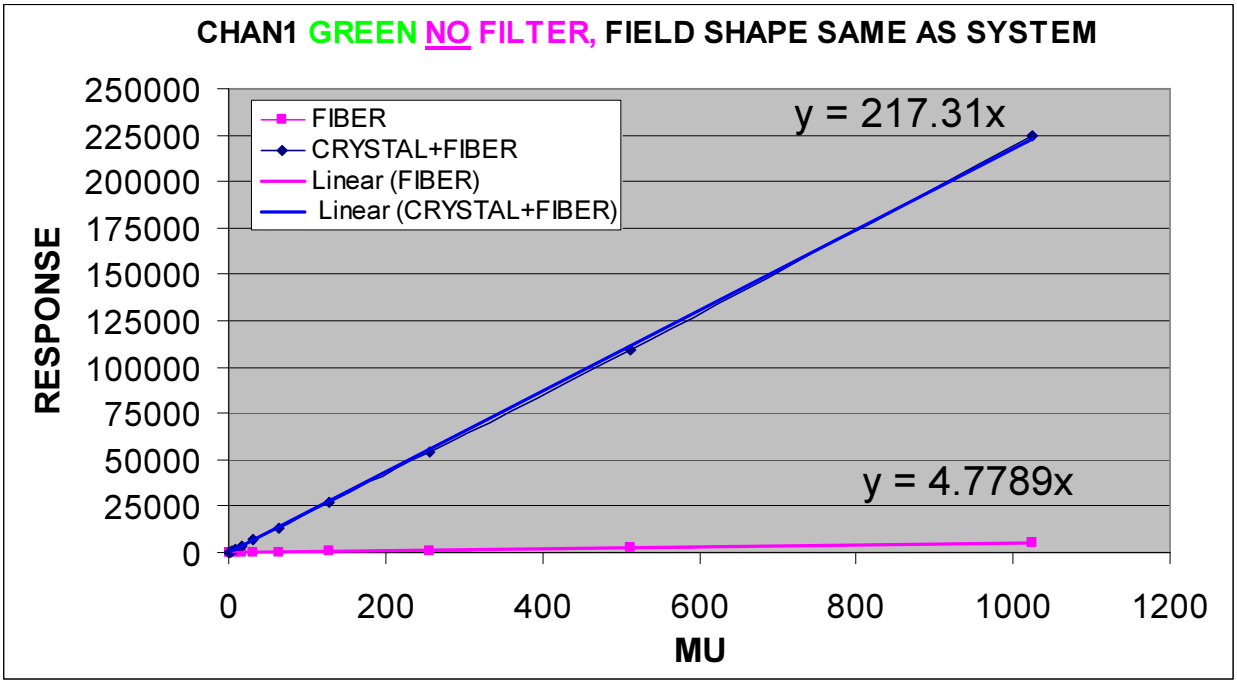

Fig 20: Plot Result of Part 2 for green system with NO filter. Field size is X=1cm, Y1=5cm, Y2=1cm. Slope for fiber and main signal are 4.7789 and 217.31 respectively. SOBR is 45.48

Table 11: Result of Part 2 for green system WITH filter. Field size is X=1cm, Y1=5cm, Y2=1cm.

CHAN 1 GREEN SYSTEM **WITH FILTER** FIELD SHAPE SAME AS SYSTEM								
MU	FIBER	FIBER	AVERAGE	AVG-BC	GREEN	GREEN	AVERAGE	AVG-BC
1	15	15	15	2	46	48	47	34
2	26	21	23.5	2.5	71	86	78.5	57.5
4	54	57	55.5	9.5	144	181	162.5	116.5
8	97	126	111.5	13.833333	357	351	354	256.3333333
16	200	191	195.5	11.166667	592	664	628	443.6666667
32	443	438	440.5	56.833333	1229	1279	1254	870.3333333
64	775	789	782	1	2467	2478	2472.5	1691.5
128	1636	1672	1654	21.666667	4843	4910	4876.5	3244.166667
256	3164	3170	3167	1	9659	9773	9716	6550
512	6349	6290	6319.5	18.166667	19641	19889	19765	13463.66667
1024	12695	12721	12708	9	42152	43586	42869	30170
							SOBR	1684

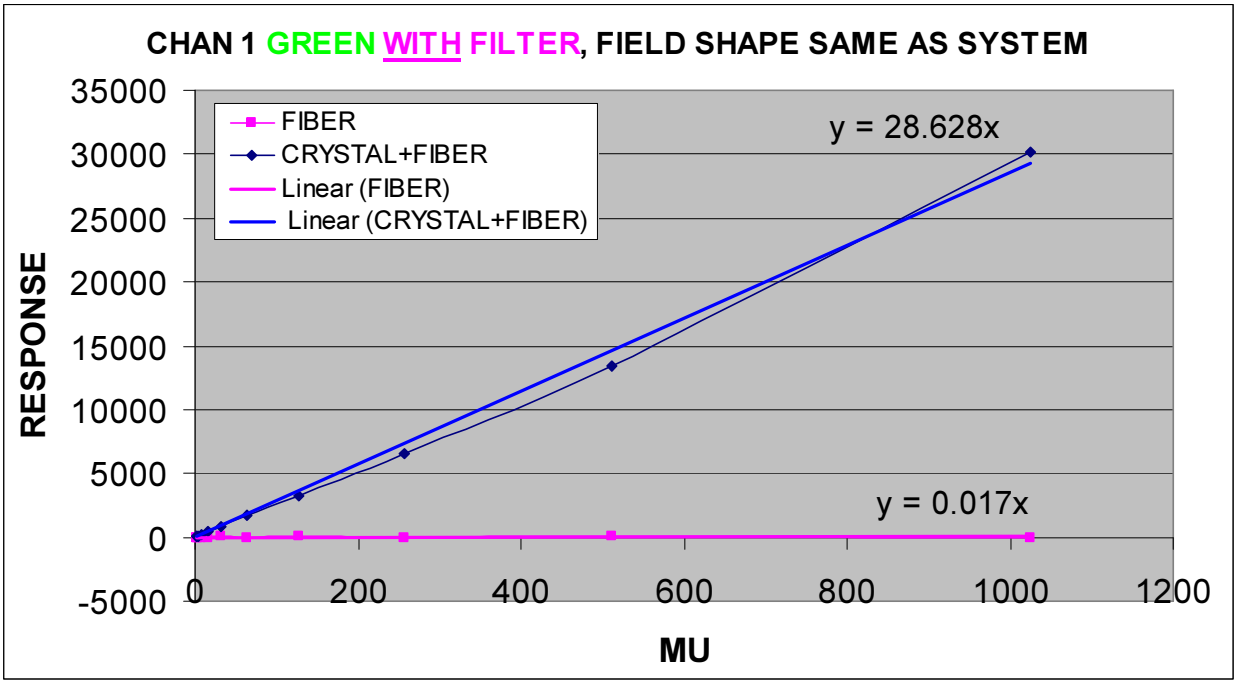

Fig 21: Plot Result of Part 2 for green system WITH filter. Field size is X=1cm, Y1=5cm, Y2=1cm. Slope for fiber and main signal are 0.017 and 28.628 respectively. SOBR is 1684

RESULTS – PART 3-1

Table 12: Result of Part 3-1 for red system with NO filter. Field size is 10x10cm^2 full field with gantry angle from -45° (315) to 45° in segments of 5°.

CHAN1 RED SYSTEM WITH **NO FILTER** 10X10 FIELD							MU = 200	
ANGLE	FIBER	FIBER	AVERAGE	AVG-BC	RED	RED	AVERAGE	AVG-BC
(315)-45	13516	13544	13530	11063.667	39333	39618	39475.5	37009.167
(320)-40	11072	10940	11006	8539.667	37902	38138	38020	35553.667
(325)-35	8886	9007	8946.5	6480.167	36838	36800	36819	34352.667
(330)-30	7296	7235	7265.5	4799.167	35582	35483	35532.5	33066.167
(335)-25	5982	5841	5911.5	3445.167	33384	33172	33278	30811.667
(340)-20	5043	5165	5104	2637.667	32467	32603	32535	30068.667
(345)-15	4233	4355	4294	1827.667	31532	31712	31622	29155.667
(350)-10	3746	3863	3804.5	1338.167	30929	30908	30918.5	28452.167
(355)-5	3405	3503	3454	987.667	30822	30759	30790.5	28324.167
0	2701	2703	2702	235.667	30231	30565	30398	27931.667
5	2601	2721	2661	194.667	30788	30830	30809	28342.667
10	2610	2619	2614.5	148.167	31065	30570	30817.5	28351.167
15	2698	2683	2690.5	224.167	31654	31480	31567	29100.667
20	2565	2613	2589	122.667	32008	31953	31980.5	29514.167
25	2533	2475	2504	37.667	32814	32499	32656.5	30190.167
30	2555	2750	2652.5	186.167	33544	33211	33377.5	30911.167
35	2791	2772	2781.5	315.167	33976	33973	33974.5	31508.167
40	2761	2812	2786.5	320.167	34719	34906	34812.5	32346.167
45	2878	2816	2847	380.667	36041	35696	35868.5	33402.167

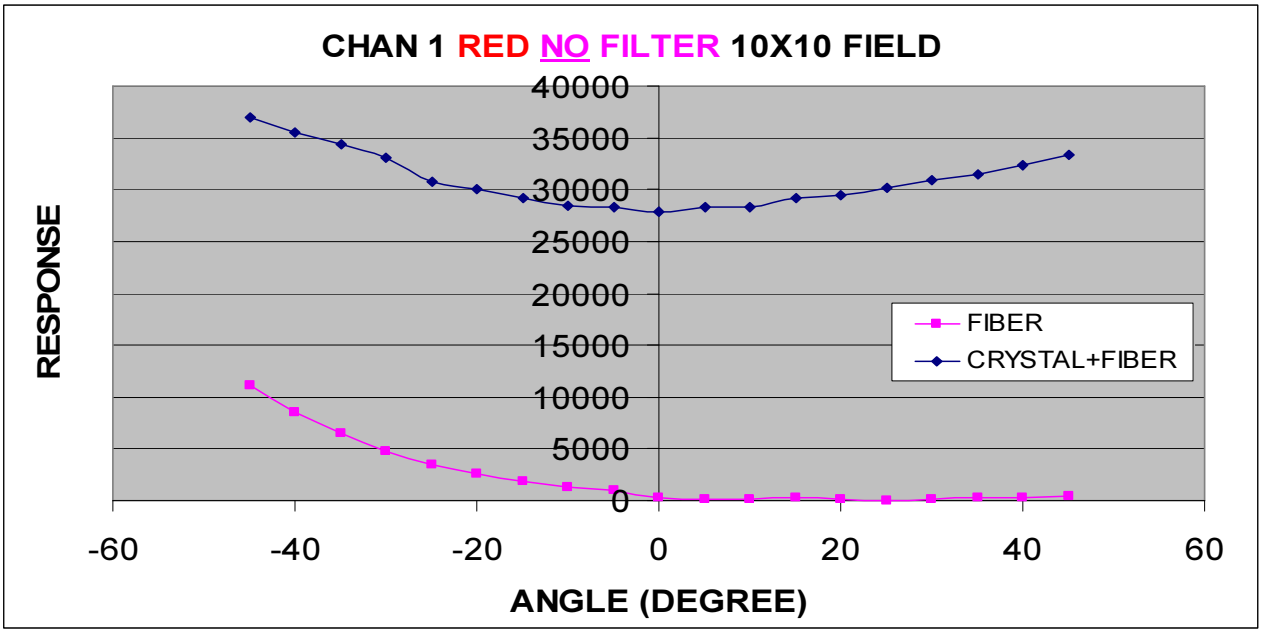

Fig 22: Plot result of Part 3-1 for red system with NO filter using 10x10 cm^2 full field. Gantry angle varies from -45° (315) to 45° in segments of 5°.

Table 13: Result of Part 3-1 for green system with NO filter. Field size is 10x10cm^2 full field with gantry angle from -45° (315) to 45° in segments of 5°.

CHAN1 GREEN SYSTEM WITH **NO FILTER** 10X10 FIELD							MU = 200	
ANGLE	FIBER	FIBER	AVERAGE	AVG-BC	GREEN	GREEN	AVERAGE	AVG-BC
(315)-45	16313	16421	16367	13829.667	48133	48362	48247.5	45710.167
(320)-40	13498	13599	13548.5	11011.167	46372	46362	46367	43829.667
(325)-35	11280	11215	11247.5	8710.167	44492	44023	44257.5	41720.167
(330)-30	9088	9059	9073.5	6536.167	42206	42215	42210.5	39673.167
(335)-25	7378	7377	7377.5	4840.167	40644	40819	40731.5	38194.167
(340)-20	6343	6114	6228.5	3691.167	39426	39176	39301	36763.667
(345)-15	5178	5410	5294	2756.667	38385	37912	38148.5	35611.167
(350)-10	4515	4353	4434	1896.667	37772	37492	37632	35094.667
(355)-5	3908	3991	3949.5	1412.167	37384	37299	37341.5	34804.167
0	3131	3159	3145	607.667	37845	37232	37538.5	35001.167
5	3040	3125	3082.5	545.167	38369	37247	37808	35270.667
10	2919	2938	2928.5	391.167	38948	37368	38158	35620.667
15	3231	3104	3167.5	630.167	39867	38372	39119.5	36582.167
20	3083	3074	3078.5	541.167	40480	39227	39853.5	37316.167
25	2994	3134	3064	526.667	41272	39956	40614	38076.667
30	2896	3091	2993.5	456.167	42400	40590	41495	38957.667
35	3038	2961	2999.5	462.167	43250	42005	42627.5	40090.167
40	3050	2975	3012.5	475.167	44822	43093	43957.5	41420.167
45	3061	2865	2963	425.667	46111	44092	45101.5	42564.167

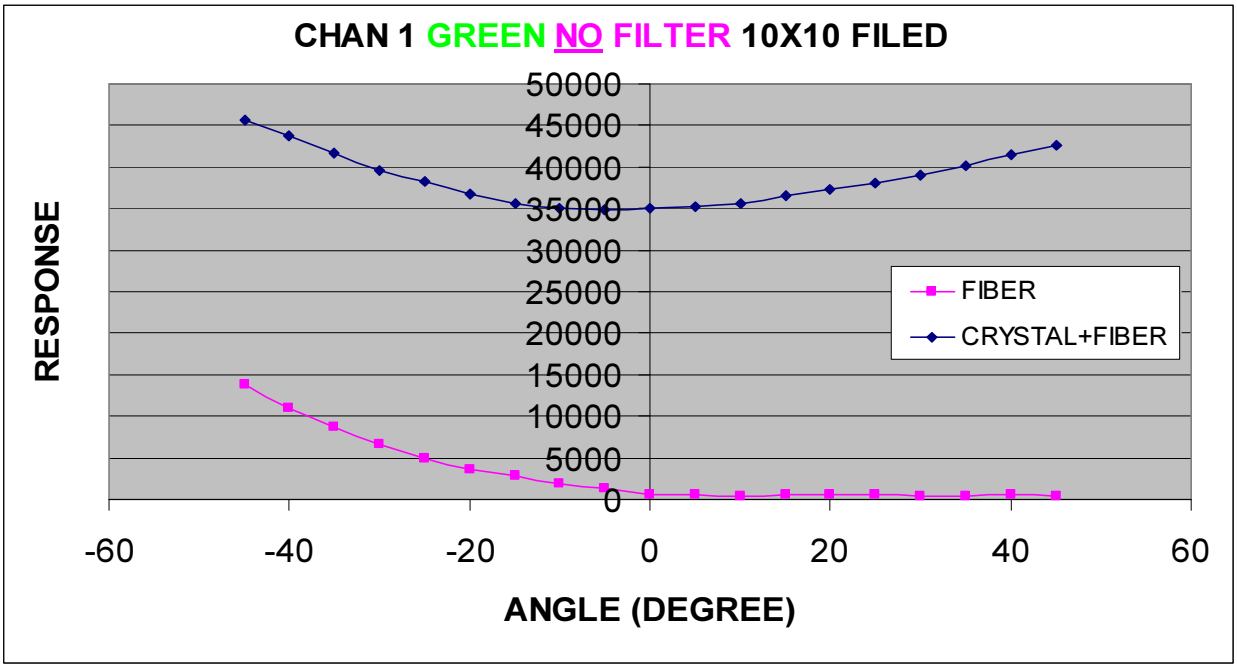

Fig 23: Plot result of Part 3-1 for green system with NO filter using 10x10 cm^2 full field. Gantry angle varies from -45° (315) to 45° in segments of 5°.

Table 14: Result of Part 3-1 for red system WITH filter. Field size is 10x10cm^2 full field with gantry angle from -45° (315) to 45° in segments of 5°.

CHAN1 RED SYSTEM **WITH FILTER** 10X10 FIELD							MU = 200	
ANGLE	FIBER	FIBER	AVERAGE	AVG-BC	RED	RED	AVERAGE	AVG-BC
(315)-45	2701	2993	2847	380.667	3504	3598	3551	1084.667
(320)-40	2729	2713	2721	254.667	3618	3475	3546.5	1080.167
(325)-35	2612	2668	2640	173.667	3495	3569	3532	1065.667
(330)-30	2566	2533	2549.5	83.167	3445	3449	3447	980.667
(335)-25	2432	2540	2486	19.667	3420	3557	3488.5	1022.167
(340)-20	2614	2660	2637	170.667	3298	3486	3392	925.667
(345)-15	2512	2563	2537.5	71.167	3319	3466	3392.5	926.167
(350)-10	2505	2394	2449.5	-16.833	3147	3412	3279.5	813.167
(355)-5	2529	2573	2551	84.667	3344	3272	3308	841.667
0	2499	2633	2566	99.667	3264	3214	3239	772.667
5	2656	2464	2560	93.667	3243	3280	3261.5	795.167
10	2500	2548	2524	57.667	3387	3453	3420	953.667
15	2526	2469	2497.5	31.167	3273	3457	3365	898.667
20	2527	2692	2609.5	143.167	3347	3538	3442.5	976.167
25	2522	2559	2540.5	74.167	3210	3372	3291	824.667
30	2516	2498	2507	40.667	3560	3499	3529.5	1063.167
35	2546	2525	2535.5	69.167	3389	3369	3379	912.667
40	2410	2386	2398	-68.333	3471	3646	3558.5	1092.167
45	2475	2579	2527	60.667	3543	3469	3506	1039.667

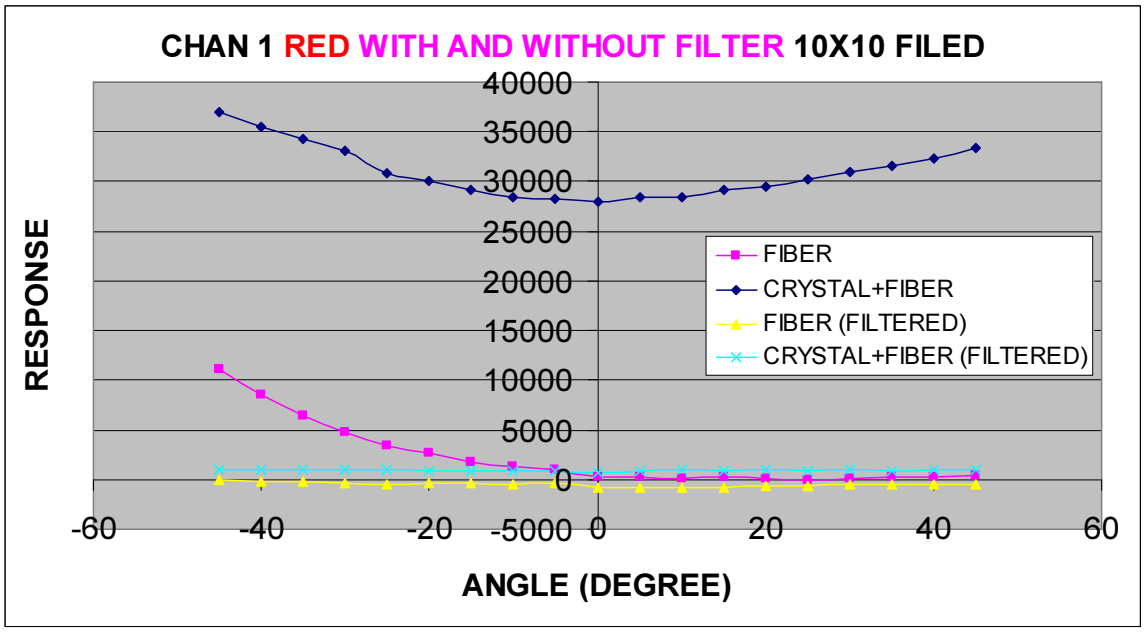

Fig 24: Plot result of Part 3-1 for red system WITH AND WITHOUT filter using 10x10 cm^2 full field. Gantry angle varies from -45° (315) to 45° in segments of 5°. From this graph you can see the comparison between the filtered and non-filtered data.

Table 15: Result of Part 3-1 for green system WITH filter. Field size is 10x10cm^2 full field with gantry angle from -45° (315) to 45° in segments of 5°.

CHAN1 GREEN SYSTEM **WITH FILTER** 10X10 FIELD							MU = 200	
ANGLE	FIBER	FIBER	AVERAGE	AVG-BC	GREEN	GREEN	AVERAGE	AVG-BC
(315)-45	3114	3113	3113.5	576.167	7327	7606	7466.5	4929.167
(320)-40	2847	2942	2894.5	357.167	7205	7282	7243.5	4706.167
(325)-35	2921	2887	2904	366.667	6907	6970	6938.5	4401.167
(330)-30	2756	2911	2833.5	296.167	6455	6451	6453	3915.667
(335)-25	2715	2709	2712	174.667	6371	6162	6266.5	3729.167
(340)-20	2652	2700	2676	138.667	6195	6076	6135.5	3598.167
(345)-15	2605	2595	2600	62.667	6049	6171	6110	3572.667
(350)-10	2595	2521	2558	20.667	6126	5950	6038	3500.667
(355)-5	2513	2527	2520	-17.333	5752	6022	5887	3349.667
0	2434	2378	2406	-131.333	4656	4505	4580.5	2043.167
5	2482	2599	2540.5	3.167	4669	5028	4848.5	2311.167
10	2414	2517	2465.5	-71.833	5151	5336	5243.5	2706.167
15	2379	2505	2442	-95.333	5256	5284	5270	2732.667
20	2446	2422	2434	-103.333	5432	5443	5437.5	2900.167
25	2442	2522	2482	-55.333	5730	5751	5740.5	3203.167
30	2526	2385	2455.5	-81.833	6208	6385	6296.5	3759.167
35	2601	2616	2608.5	71.167	6540	6539	6539.5	4002.167
40	2460	2488	2474	-63.333	6632	6640	6636	4098.667
45	2462	2530	2496	-41.333	6893	7103	6998	4460.667

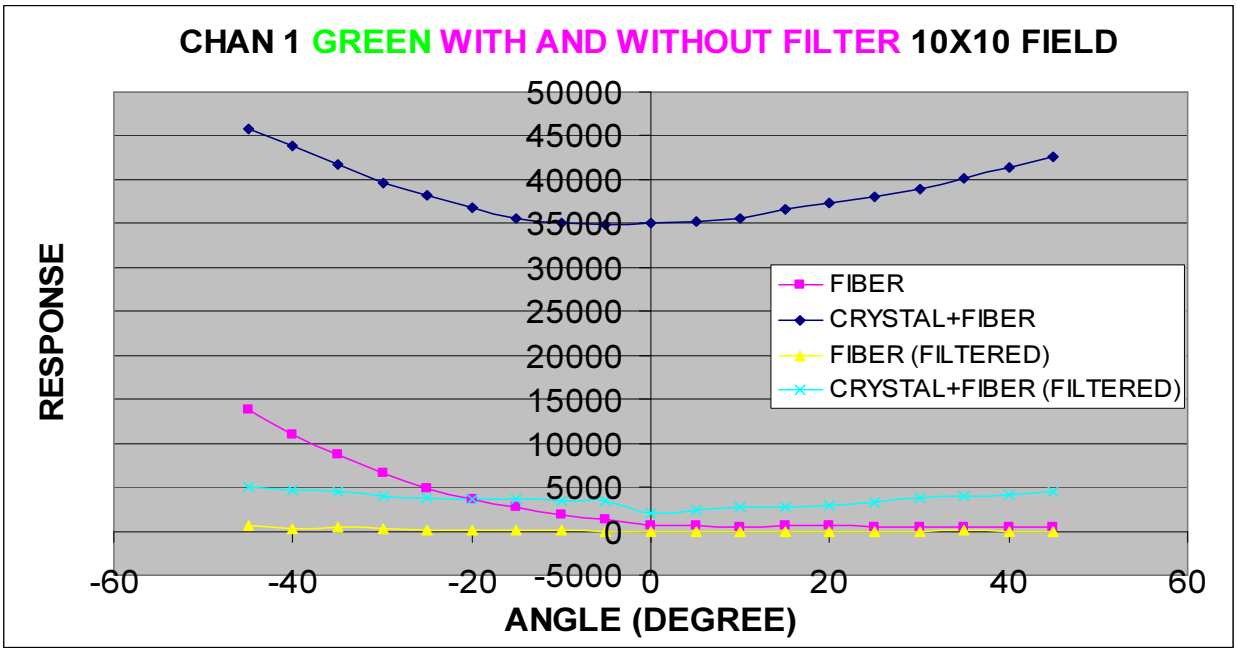

Fig 25: Plot result of Part 3-1 for green system WITH AND WITHOUT filter using 10x10 cm^2 full field. Gantry angle varies from -45° (315) to 45° in segments of 5°. From this graph you can see the comparison between the filtered and non-filtered data.

RESULTS – PART 3-2

Table 16: Result of Part 3-2 for red system with NO filter. Field size is 10x10cm^2 full field with gantry angle from -90° (270) to 90° in segments of 5°. The crystal is now pointing in the direction of the gantry.

MU=200				
CHAN1 RED SYSTEM WITH **NO FILTER** 10X10 FIELD				
ANGLE	RED	RED	AVERAGE	AVG-BC
(270)-90	28557	28568	28562.5	26096.167
(275)-85	28688	28711	28699.5	26233.167
(280)-80	28783	28564	28673.5	26207.167
(285)-75	28481	28730	28605.5	26139.167
(290)-70	28760	28653	28706.5	26240.167
(295)-65	28134	28794	28464	25997.667
(300)-60	28644	28785	28714.5	26248.167
(305)-55	28855	28781	28818	26351.667
(310)-50	28823	28900	28861.5	26395.167
(315)-45	28731	28830	28780.5	26314.167
(320)-40	29071	28823	28947	26480.667
(325)-35	28708	28728	28718	26251.667
(330)-30	28772	28885	28828.5	26362.167
(335)-25	28529	28703	28616	26149.667
(340)-20	28525	28471	28498	26031.667
(345)-15	28338	28569	28453.5	25987.167
(350)-10	27813	28190	28001.5	25535.167
(355)-5	27866	27916	27891	25424.667
0	26613	26672	26642.5	24176.167
5	26752	27090	26921	24454.667
10	27089	27087	27088	24621.667
15	27064	27019	27041.5	24575.167
20	26849	26859	26854	24387.667
25	27166	26924	27045	24578.667
30	26924	26782	26853	24386.667
35	26716	26877	26796.5	24330.167
40	26737	27055	26896	24429.667
45	26574	26798	26686	24219.667
50	26611	26763	26687	24220.667
55	26568	26544	26556	24089.667
60	26622	26420	26521	24054.667
65	26524	26366	26445	23978.667
70	26596	26608	26602	24135.667
75	26512	26898	26705	24238.667
80	26758	26699	26728.5	24262.167
85	26514	26479	26496.5	24030.167
90	26621	26737	26679	24212.667

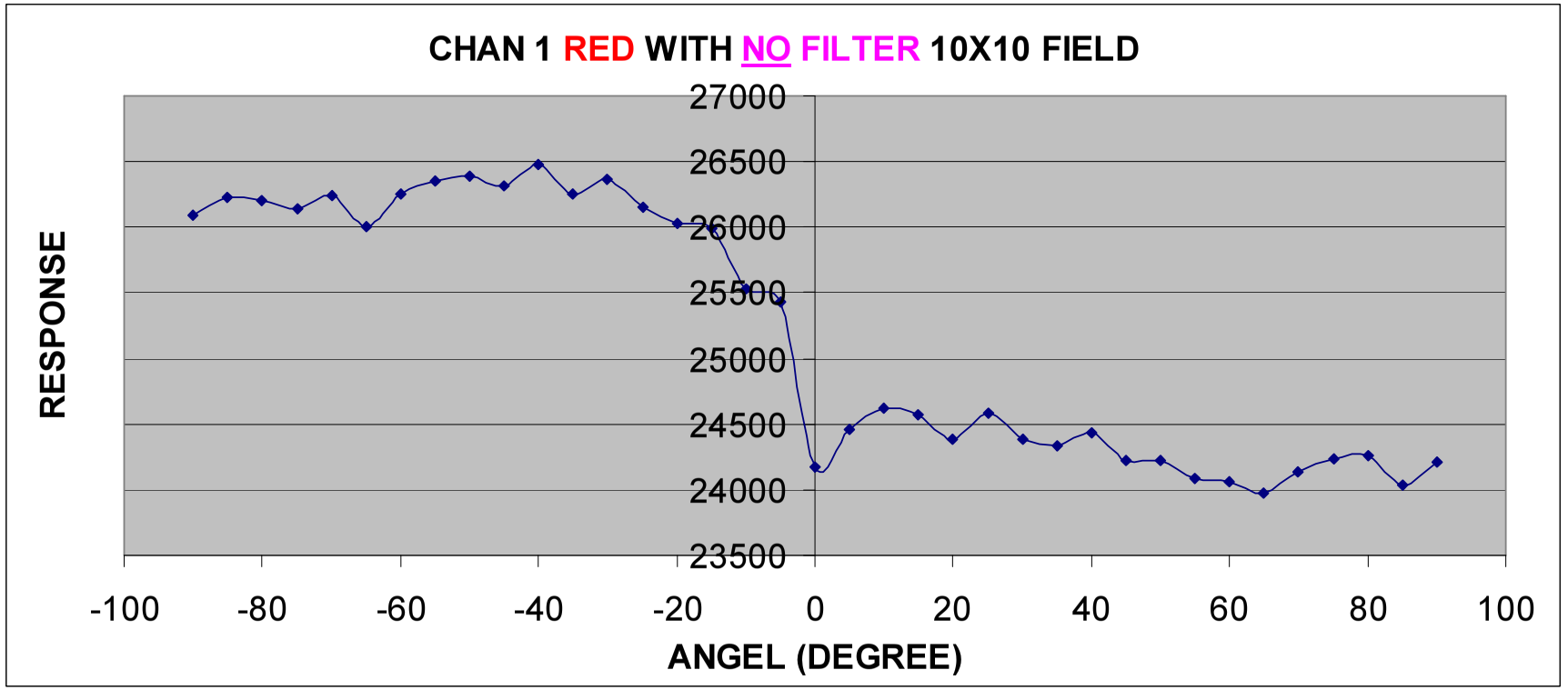

Fig 26: Plot result of Part 3-2 for red system with NO filter using 10x10 cm^2 full field. Gantry angle varies from -90° (270) to 90° in segments of 5°. The crystal is pointing in the direction of the gantry.

Table 17: Result of Part 3-2 for green system with NO filter. Field size is 10x10cm^2 full field with gantry angle from -90° (270) to 90° in segments of 5°. The crystal is now pointing in the direction of the gantry.

CHAN1 GREEN SYSTEM WITH **NO FILTER** 10X10 FIELD				
ANGLE	GREEN	GREEN	AVERAGE	AVG-BC
(270)-90	42440	42269	42354.5	39817.17
(275)-85	42150	41979	42064.5	39527.17
(280)-80	41937	42050	41993.5	39456.17
(285)-75	42289	41920	42104.5	39567.17
(290)-70	41922	42179	42050.5	39513.17
(295)-65	41804	41841	41822.5	39285.17
(300)-60	41630	41919	41774.5	39237.17
(305)-55	41791	41583	41687	39149.67
(310)-50	41442	41884	41663	39125.67
(315)-45	41742	41032	41387	38849.67
(320)-40	41897	41749	41823	39285.67
(325)-35	41863	41420	41641.5	39104.17
(330)-30	42025	41729	41877	39339.67
(335)-25	41569	41634	41601.5	39064.17
(340)-20	41614	42006	41810	39272.67
(345)-15	41742	41757	41749.5	39212.17
(350)-10	41824	41869	41846.5	39309.17
(355)-5	41912	42303	42107.5	39570.17
0	41768	42023	41895.5	39358.17
5	41895	41896	41895.5	39358.17
10	42168	41839	42003.5	39466.17
15	41944	42135	42039.5	39502.17
20	42073	41876	41974.5	39437.17
25	41916	41895	41905.5	39368.17
30	42026	42049	42037.5	39500.17
35	41585	41851	41718	39180.67
40	41686	41564	41625	39087.67
45	41368	41945	41656.5	39119.17
50	41612	41942	41777	39239.67
55	41725	41843	41784	39246.67
60	42012	41725	41868.5	39331.17
65	41917	41890	41903.5	39366.17
70	41778	42149	41963.5	39426.17
75	41999	42074	42036.5	39499.17
80	41959	42033	41996	39458.67
85	41987	42053	42020	39482.67
90	42029	41867	41948	39410.67

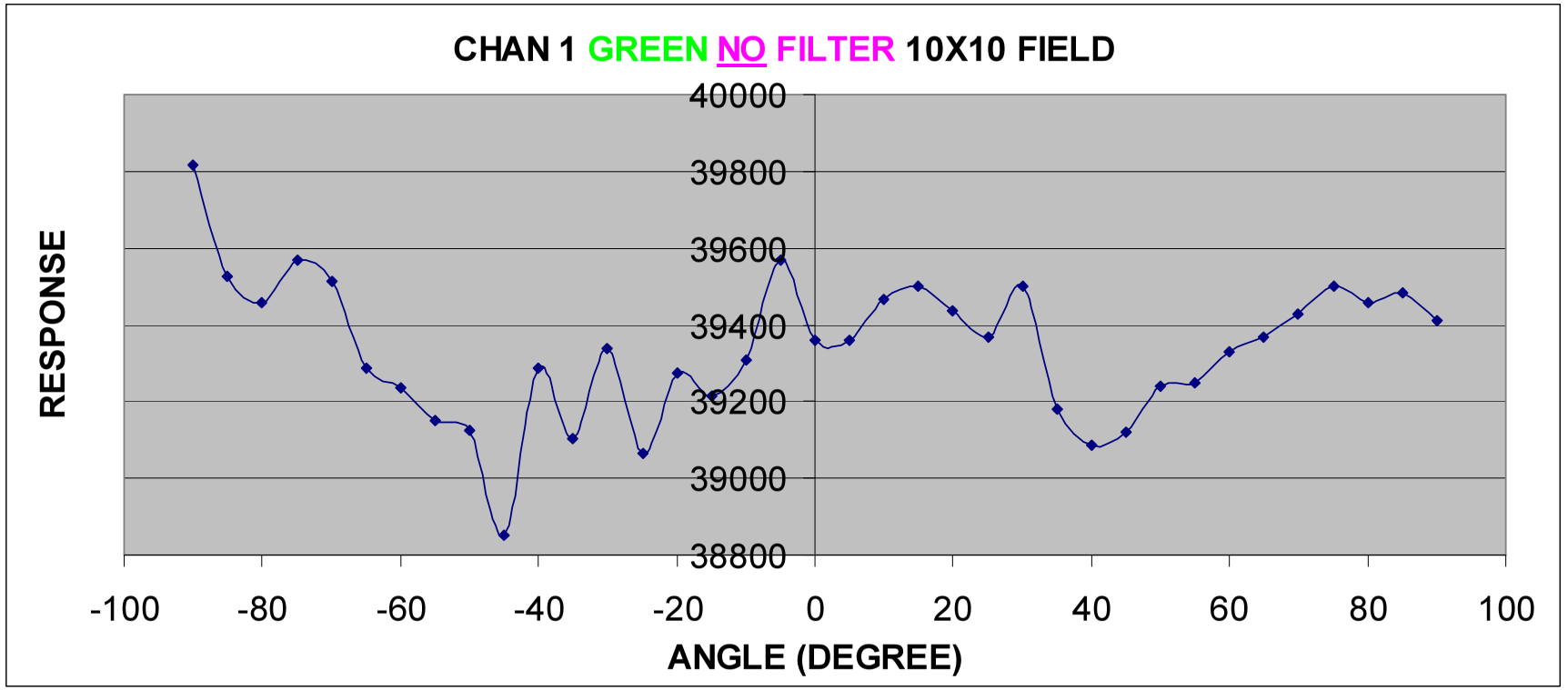

Fig 27: Plot result of Part 3-2 for green system with NO filter using 10x10 cm^2 full field. Gantry angle varies from -90° (270) to 90° in segments of 5°. The crystal is pointing in the direction of the gantry.

DISCUSSION – Part 1

We first note that the dark counts scaled linearly with the MU's (plots not shown). The dark counts are probably not thermally generated, but caused the EMF noise associated with the linear accelerator. The red and green channels had nearly the same dark counts, with a slight increase in the green channel. The slight difference between the two channels can well be attributed to subtle differences in the electronic components used in the two channels.

We had initially thought the subtraction routine used in the integrator box would eliminate any dark counts. In fact, the integrator circuit does eliminate nearly all the thermally generated dark counts. The large number of dark counts that are associated with the EMF noise is troubling. This subtraction contributes to large uncertainties in the measurements.

One of the major cause of the noise is actually the LINAC itself. When the LINAC is beam on, it generates a lot of noise due to high energy emission. The noise will affect all the electronics around the LINAC. In the hospital, there are 3 LINACs in the oncology department. This makes the working environment very noisy. The term "noisy" does not refer to the noise we hear, but the noise that gets into the electronics and interferes with it.

The noise can not be eliminated. A more professional level of components and shielding for our electronics will need to be used for the apparatus to be improved. These components include op-amp, integrator, ADC, leads and so on.

The dark counts are not dependent on our experimental set up. They only depend on the MU. Different MU will have different dark counts. No matter how big the field size is, or what kind of shape of field you have, as long as the MU is the same, the dark counts will be the same. Also, adding the optical filter to the system does not affect the dark counts either. This tells us the dark counts are not coming from the scintillator crystal or the fiber. It is the LINAC pulse trigger output that sends the pulses to our electronics box which then generates the dark count.

Table 18: Summary of the system response slope from Part 1 and Part 2 of the methods.

Scintillator	Optical Filter	Response Slope (counts/MU)		SOBR	Optical Filter Attenuation (%)	
		Crystal +Fiber	Fiber		Crystal +Fiber	Fiber
20x20 Half Field						
Red	Without	239.95	14.48	16.58		
	With	8.27	0.75	11.03	3.45	5.18
Green	Without	291.22	16.41	17.75		
	With	39.11	0.59	66.72	13.43	3.57
1x5 Shaped Field						
Red	Without	182.43	4.11	44.43		
	With	6.85	0.44	15.62	3.76	10.68
Green	Without	217.31	4.78	45.47		
	With	28.63	0.02	1684	13.17	0.36

In Part 1, we use a 20x20cm^2 half field to irradiate the scintillator crystal with fiber, and fiber alone. For each MU we make the measurement twice and take the average. Then we subtract the dark counts from the average value that corresponds to each MU. No matter whether we are dealing with the data of "Fiber" or "Fiber + Crystal", the dark counts are the same for both cases. The reason is because this noise is always there, no matter what is irradiated. The noise is generated from the surrounding electronics.

From the readings in our charts we see that the red green scintillators gave nearly the same size signals. The slope of the red signal without filter was 240 counts per MU. The slope of the green signal was 291 counts per MU. This is somewhat surprising, because the red crystal does not have as high a light output as the green crystal.

From the data sheets, we learn that the light output is only 45% for the red crystal and 60% for the green crystal. We would expect the green scintillator to provide 1.33 times more signal than the red. Instead, we saw on 291/240 = 1.21 increase.

There are several reasons that this ratio is less than 1.33. The most likely reason is the attenuation of the plastic fibers. They attenuate shorter wavelengths more than longer wavelengths. With more than 25 meters of fiber in both paths, the attenuation difference could explain lack of green signal.

To have a more detailed look at our results, we plot the final data from "Fiber" and "Crystal + Fiber" signals. The graph shows two straight lines. This means the system is linear. When we double the MU, the response should double. This is an essential property that any dosimetry system must have. Microsoft Excel can calculate the slope (gradient) of these two lines for us very easily by using the "add trend line" option. We also forced the fit to pass through the origin, acknowledging that there should be no signal when the accelerator is off. We simply divide the two gradients and find the SOBR.

From the graph you will see the title reads "CHAN 1 RED NO FILTER 20X20 HALF FILED". The reason it shows "CHAN 1" is because in our electronic box, there are two channels. In the beginning, we were intending to have the red system in channel 1 and the green system in channel 2. But then we discovered the channels were not synchronized. Because of the offset setting, it is very hard to ensure both channels have exactly the same sensitivity. There will always be a ratio between two channels, so eventually we decided to use channel 1 only. Every time we perform an experiment with either system, we perform the experiment with channel 1, and the other system will be plugged into channel 2 for resting.

Because the fiber will always generate a background signal (fluorescence and Cerenkov), which will decrease the SOBR, a way to improve it is to add an optical filter to the system. This filter needs to be selected from the manufacturer to match the signal wavelength. The red scintillator crystal gives out light with a wavelength of 580nm. Our optical filter has a center wavelength of 585nm with a bandwidth of 10nm ± 1. This should cover the wavelength that the crystal is giving out.

From our results, we see that both “Fiber” and “Crystal + Fiber” signals have reduced when the optical filter is added. The slope of the signal decreased from 240 to 8.3. The filter only transmitted 3.5% of the signal. This is unreasonably small. The optical background slope decreased from 14.5 to 0.8 or a reduction of 5.2%. Thus, the SOBR was actually made worse by the addition of the optical filter. We suspect that either the bandpass of the filter is not centered at 585nm or the scintillator output is not centered at 580nm. We have sent both of these optical elements to be checked by a calibrated optical laboratory.

With the green system, when no optical filter was added, the signal from the crystal and fiber has slope of 291 counts per MU. This is 21% greater than the red scintillator. The “Fiber” has a slope of 16.4 counts per MU. This is 13% greater than the red scintillator. To first order, one would expect the “Fiber” signal to be independent of the crystal. We did not see that. The SOBR without the filter of both red and green systems are similar. The green has the SOBR of 17.7 compared to the red system of 16.6.

When we added the optical filter to the green system, the story became completely different. We found the “Fiber” signal is very much reduced, from a slope of 16.4 counts/MU to 0.6 counts/MU. This “Fiber” response is even less than the red system. The filter also worked very well for the scintillator crystal itself. The filter removed a lot of signal from the crystal. The slope of the response decreased from 291 to 39.1. Thus, 13.4% of the signal passed through the filter. Although, that is small percentage, it is reasonable. Using the green optical filter gives us a SOBR of 67.

A SOBR of 67 can also be expresses as 1.5% optical background signal in the measured reading. Thus, in this geometry of a 90˚ radiation exposure, the green scintillator crystal with the optical filter can be used as a dosimetery with a 1.5% uncertainty in the measured dose.

Part 2

In Part 1, we performed the experiment using a 20x20 cm^2 half field. Now we will change the field shape to the same as the outline of the system. The rest of the set-up is exactly the same as Part 1. The field shape set-up is X=1cm, Y1=5cm and Y2=1cm according to the LINAC jaws setting.

The reason for doing this is to see how this field shape will perform differently from the 20x20 cm^2 half field. We discover that the reduced field shape gives us a higher SOBR. If we look at the data without using a filter, the response for both "Fiber" and "Crystal + Fiber" are less than using the 20x20 cm^2 half field. This happens to both red and green systems. The major issue is that the background signal, or the "Fiber" signal. It is decreased a lot. The "Crystal + Fiber" signal is decreased by less. The biggest difference happens to the "Fiber" signal. This raises the SOBR for both systems, especially the green system.

We would expect that a smaller field size would give a decreased signal because there is less signal from scattered photons. The scattered photons would preferentially add to the fiber signal over the crystal signal. This is because of the length of the fiber and the orientation of the fiber. As explained below, the photons are not oriented for maximum Cerenkov production that will couple down the optical fiber. However, scattered photons will likely to be a more favorable direction to couple down the fiber. Decreasing the scattered photons by decreasing the field size gives the expected increase in SOBR.

When the optical filter is added to both systems, the "Fiber" signal decreases even more. This will raise the SOBR even further. The green system with filter has the SOBR equal to 1684. The cause of this is that when the field is narrowed to the size of the system, which is only 1cm wide and 6cm long, it reduces the scattering even more. It does not have as great of an impact on the crystal.
So we only see a little decrease in effect on signal for the crystal. When we add an optical filter, it further reduces the optical background (the "Fiber" signal), so we have an even higher SOBR than without an optical filter

Part 3–1

In this part of the experiment, we want to test the directional response of the scintillator detector. We fire the radiation from different angles by rotating the gantry of the LINAC and see how the detector will respond. There is one thing in this experiment set-up that is different to part 1 and part 2. That is that we do not use a solid water block. This is because as we start to change the beam angle, the area of the field on the flat surface of the solid block water will change. So, the amount of back scatter will be different for each different angle. This will confound the measured response as the beam angle changes.

From the graph we've plotted for the green system, we can see that when the radiation is coming from a steeper angle, the response is higher. The same effect happens for both positive and negative angles. This is because as the beam is coming from a steeper angle, the Cerenkov effect will start to contribute to the system. To understand this, we need to do a simple calculation.

The calculation is this:

First we find the Critical Angle of the fiber. We use the refractive index of the core and the clad to do this:

$$\theta c = Sin^{-1}\frac{n_2}{n_1}$$

$$\theta c = Sin^{-1}\frac{1.402}{1.492}$$

$$\theta c \approx 70°$$

θc = Critical Angle
n_1 = Refractive Index of Core
n_2 = Refractive Index of Clad

Now we need to find the maximum Cerenkov Angle that will happen inside the fiber:

$$Cos\theta_{Cerenkov\max} = \frac{1}{n_1}$$

$$Cos\theta_{Cerenkov\max} = \frac{1}{1.492}$$

$$\theta_{Cerenkov\max} \approx 48°$$

Here is a diagram to show what happens in the fiber:

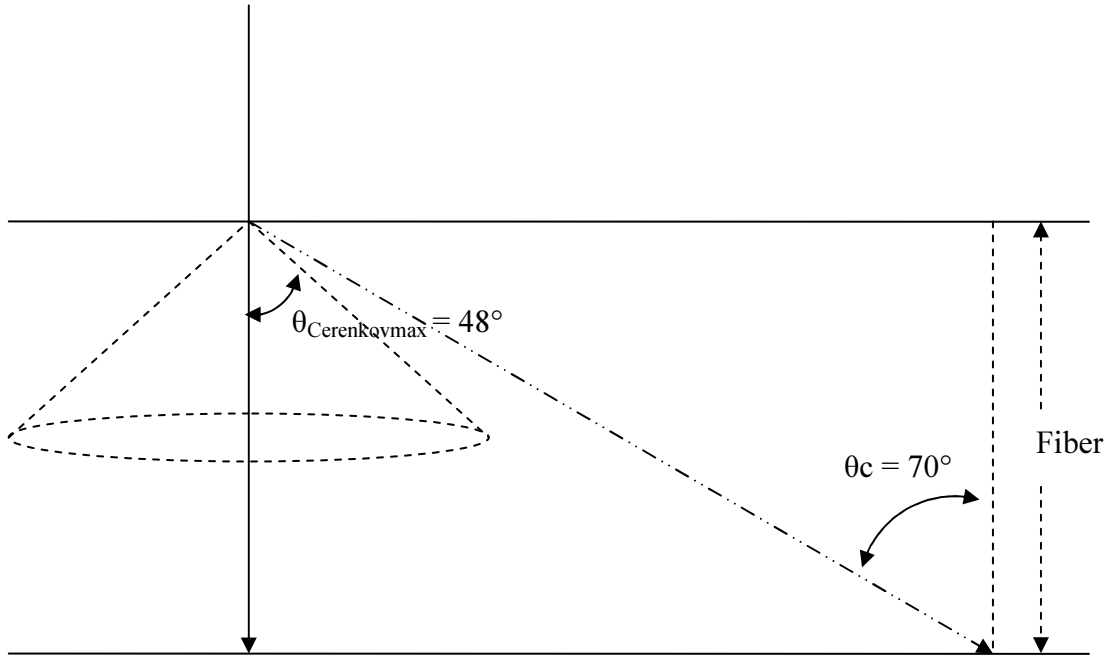

Fig 28: When the radiation beam is perpendicular to the fiber, the Cerenkov cone appears in an upright position inside the fiber. In our case the Cerenkov cone has an angle of 48° and the critical angle is 70°.

This is the situation when the radiation beam is perpendicular to the fiber. There are two main background signals created by the fiber, fluorescence and Cerenkov radiation. Cerenkov radiation appears as a cone.

The angle of the cone is dependent on the core refractive index of the fiber. The higher the core refractive index, the bigger the angle of the Cerenkov cone. In our case, the core refractive index is 1.492 - this gives us the Max Cerenkov angle of approximately 48°. The critical angle of the fiber is about 70°. From the specification of the fiber, we are told that the fiber has an acceptance angle of 61°. We can also calculate the 61 degree acceptance angle using the 70 degree critical angle and Snell's law.

If we start to change the beam angle, the story will be different. As the beam angle changes, the Cerenkov cone will start to rotate, this will affect the response of our detector.

Here is a diagram to illustrate what happens inside the fiber:

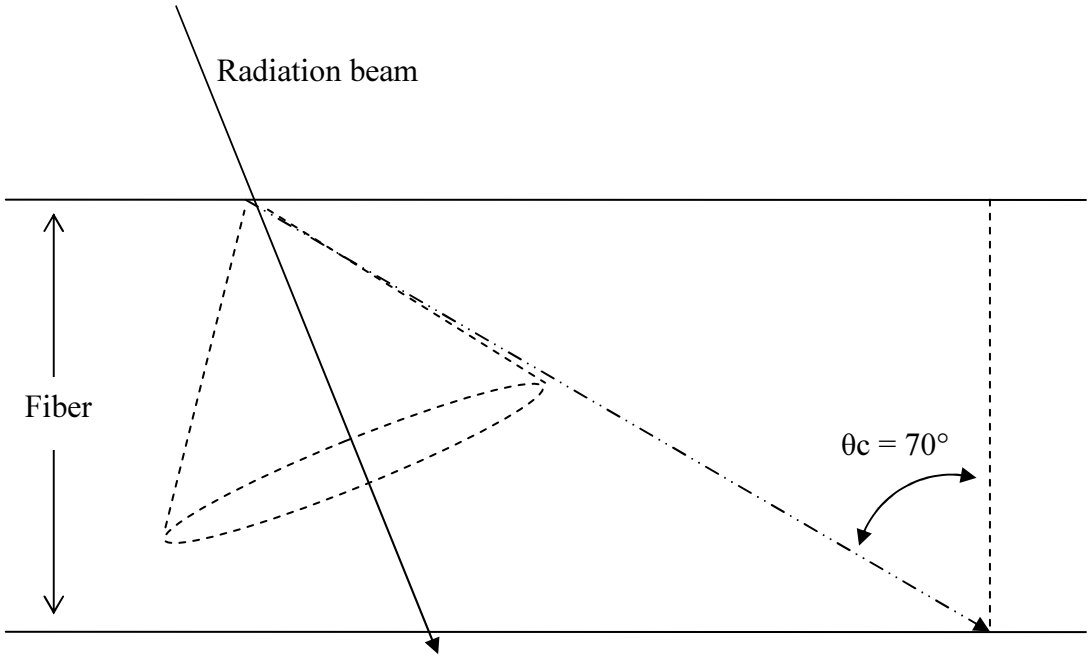

Fig 29: When we start to change the angle of the radiation beam (by changing the gantry angle), the Cerenkov cone will change its angle corresponding to the beam. When the angle of Cerenkov meets the critical angle, an increase in response will be observed.

You can see that if the beam angle is changed, the cone will rotate with the beam. The cone will eventually reach the critical angle and even pass it.

So when the beam is perpendicular to the fiber, no Cerenkov radiation from the direction of the primary photons will contribute to the reading. Because the Cerenkov angle is smaller than critical angle for the direction of the primary photons, the Cerenkov radiation does not couple down the fiber and reach to the photodiode.

As the beam angle changes, Cerenkov will get closer to the critical angle. Once it has reached the critical angle, Cerenkov will start contribute to the result. The starting point of this effect is when the angle of the beam reaches the difference of critical angle and Cerenkov, which will be 22°. This means when the beam angle reaches -22° the response of the detector will increase, because Cerenkov will be present at all angles beyond -22°. We note that -22˚ is the radiation directed towards the distal end of the fiber. We do not expect to see an increase in the Cerenkov radiation at 22˚ and larger angles, because this is directed away from the detector and will cause the light to couple down the optical fiber away from the detector.

From the fiber alone without using the optical filter, the signal does increase at more negative angles than -22˚. In fact, the increase in signal could start at -12˚. This would be consistent with the stated acceptance angle of 61˚ for the plastic optical fiber. The response is flat for angles greater than 0˚.

Looking at the “Crystal + Fiber” signal, without the optical filter, we see the signal increases for both positive and negative angles. This was not expected. The increase in the signal with negative angles is expected. It is simply the Cerenkov radiation as we explained above. The increase in the signals with the positive angles is due to the short wavelength radiation (e.g., blue light) from Cerenkov and fluorescence processes in the fiber coupling down the fiber and being transmitted to the scintillator crystal. The crystal will absorb this visible light and fluoresce green.
The green fluorescence occurs in all directions. Some of this fluorescence from the Cerenkov light and optical fiber fluorescence will couple towards the detector and create a signal.

Our graph is consistent with our revised expectations. The signal increases as the angle of the beam changes. But there is a difference of response between the “Fiber” signal and the “Crystal + Fiber” signal. If we look at the green system with no filter

first, it is showing a higher response on the negative side of the angle for both “Fiber” and “Crystal + Fiber” signal. The response of “Fiber” stays roughly constant when the beam angle is positive. At angle 0° to 45°, the beam is pointing in the direction of the scintillator crystal. Because the point where we irradiate the fiber is some distance away from the crystal, light generated by the fiber will have two different paths to reach the photodiode. Both paths will begin at the point of the fiber where the interaction occurs. The first path will go directly from the point of interaction to the photodiode. The second path will go from the point of interaction to the crystal. In the crystal the light will cause the dye to optically fluoresce. This fluorescent is emitted in all directions, so some will travel through the fiber to the photodiode. Most light will be traveling the second path due to the direction of the beam. This longer distance travel will cost attenuation, therefore weakening the signal. But still a small percentage of light will travel the first path.

When the gantry is at 0° to -45° (315°), the beam is pointing in the direction of the photodiode. In this case, almost all of the light that is created can reach the photodiode directly from the point in the fiber where interaction occurs. Therefore, the response of the system will be higher when the gantry angle is at negative, which is confirmed by our graph.

But this effect is not as clear with the “Crystal + Fiber” signal. We can still see the response of the positive angles is less than the response of the negative angles, but only a little bit. The response does not stay constant at positive angles like the “Fiber” signal. The response of “Crystal + Fiber” at the positive angles increases with angle, unlike the “Fiber” signal that remains near zero. This is explained by the light from the fiber being converted to green and red light in the green or red crystal, respectively. This converted light then travels to the detector. When there is no crystal, the background light traveling in the wrong direction is simply lost to attenuation in the optical fiber.

To sum up this part of the investigation is when the gantry angle is at positive, most of the light created during interaction inside the fiber will travel in the direction towards the scintillator. This background light will make the scintillator optically fluoresce.

We previously thought the total light from scintillator crystal was from the interaction of the ionizing radiation beam. But actually, part of scintillator light is created from the optical conversion of the Cerenkov and fluorescence light created in the fiber. This extra scintillator light gives us the increasing signal of "Crystal + Fiber" at positive irradiation angles. Our optical filter is located at the distal end of the fiber, where it is impossible to eliminate this extra light.

As for the "Crystal + Fiber" signal, we see the increase in response on both sides, because no matter how we change the gantry angle, the interaction is always happening inside the crystal. This means there is only one path for light to reach the photodiode - that is the "first path" that we've mention previously. Therefore, the issue of light traveling an extra distance to reach the photodiode does not arise. When the gantry is at 0° to -45° (315°), light will launch straight to the photodiode because the direction is matched. When the beam is coming from 0° to 45°, a portion of the light will need to travel to the crystal and optical fluorescence in the crystal can then be launched to the photodiode. The light is attenuated long before it can travel this distance.

This extra distance that the light needs to travel when the crystal is in the field is very small. But we can still detect the difference in our result. The peak response on the negative angles is higher than the positive angles.

When the optical filter is placed in the system, the response might appear to be flat. However, it differs by a factor of two between 0° and ±45°. Thus, the SOBR approaches 1.0 at ±45°. This is an unacceptably low value for the SOBR.

Part 3 – 2

This part of the experiment is similar to Part 3-1. The only difference is we place the crystal pointing the direction of the gantry of the LINAC. We irradiated the crystal with beam angle varies from -90°(270°) to 90° and see how the detector will respond. This is purely to test the directional response of our system. Because the crystal is pointing in the direction of the gantry, no matter which angle the beam is coming from, there will only be one path for light to reach the photodiode.

Therefore, this method can really tell us how our system responds to the radiation beam that comes from various angles.

From the plot we have for the green crystal, it is actually showing a good result. The result shows us the response is oscillating up and down. This is very normal. An ideal result would be a straight horizontal line, because we want an equal response and sensitivity at all angles. But in real life, this is not going to happen due to noise. But if we look at it carefully, even thought we don't get a straight line, the difference between the highest point and the lowest point is only 2.5%. This is a very minimal error which can be accepted.

As for the red system, the responses for both the positive and negative angles are more consistent. But notice the response is higher on the negative angles than the positive. The point of this change starts near 0°. The response suddenly changes approximately 9%. The main reason is thought to be due to the cement we used to attach the crystal to the fiber. The cement must be very uniformly laid on the surface of both the crystal and the fiber. The amount and the thickness must be exactly the same through the whole surface.

Likewise, the surface of the optical fiber and crystal must be polished to very smooth and flat surfaces. This is very difficult to achieve. If the cement is not uniformly laid or the surfaces are not well polished, it will affect the result.

Another factor affecting our results is the dark counts. We've recorded all the dark counts corresponding to different MU. But because dark counts are noise, they also vary. Every time we measure them, they are a little different. This means the dark counts also vary. If dark counts change, so do our results. This is why the results for Part 3-2 appears to have so much noise.

There are two important factors in this research project that really affected the result. The first factor that can be improved is the crystal. We've notice during the research, if we keep irradiating the crystal, that the response seemed to increase a little bit. So we suspect that the crystal is actually heating up.

If the crystal is used *in vivo* or inside a living patient, the person would act as a "heat sink" and maintain the temperature near 37˚.

The second factor is our electronics. The electronics for integration should be made more precise and professional. This would give us a more accurate read out. Because the components we have used for the electronics part are consumer level, they actually contain many problems. For example: the shielding, the gain level, dependence of channels 1 and 2, sensitivity of the photodiode, and many more. The electronics are actually very important in this research project.

Lastly, we have mentioned in Part 3-1 that for when the gantry is at the positive angle for "Crystal + Fiber" signal, the conversion of Cerenkov and fluorescence to scintillator light will happen. This is impossible to eliminate in our system. So a new system will need to be designed to eliminate the background signal in both directions. One possibility would be to build an optical filter at the interface between the fiber and crystal.

CONCLUSION

In this research project, we've investigated the efficiency of red and green scintillator crystal interactions with ionising radiation in conjunction with optical fiber. The system consists of scintillator crystal, optical fiber, optical filter, plano-convex lens, photodiode and electronics for integration. In Part 1, we irradiated both of our systems with 20x20 cm2 half field beam. The beam was perpendicular to the system with MU doubled each time starting from 1MU. The SOBR for red and green system with no filter was 16.58 and 17.74 respectively. If we added the optical filter into the system, the SOBR for red and green became 11.03 and 66.72 respectively. We suspect the red optical filter or the red scintillator crystal are not performing according to specifications.

In Part 2, we change the field shape matching the outline of the system. The dimension of the field is X=1 cm, Y1=5 cm and Y2=1 cm. The beam is still perpendicular to the crystal. The SOBR for red and green system with no filter is 44.43 and 45.47 respectively. After we've added the optical filter in to the system, the SOBR for red and green become 15.62 and 1684 respectively. This is a very promising result.

From this result, we see that there isn't much difference in SOBR between the red and the green system when no optical filter is in place. The green system always tends to have a little higher SOBR than the red, because green scintillator crystal has a higher light output than the red. When we place the optical filter into the system, we can see a bigger difference between them. In both Part 1 and Part 2, the green system has shown a much higher SOBR when an optical filter is in place. We know that the optical filter will filter out both background signal and some main signal too. We suspect there is a problem in the red system.

In Part 3, we tested the response of our systems with various beam angles. To do this, we simply change the gantry angle of the LINAC. First, we place the crystal horizontally and use a beam angle range from -45° to 45°. We also tested with filter and without filter.

When an optical filter is placed in the system, the response is significantly decreased. One line represents the “Fiber” signal and the other one is “Crystal + Fiber” signal. When optical filters are removed from the system, the response for “Fiber” signal increases when the angle is negative. On the positive angles, the response is not quite as large. This is because when the beam is coming from the positive angle, light created during interaction travel in a direction opposite the photodiode. This longer distance traveled involves attenuation and signal loss. When the beam is coming from the negative angle, the direction of the beam is pointing towards the photodiode. This makes the light created during interaction launch straight to the photodiode without traveling an extra path. So the result shows an increase in response as angle increases.

Irradiation at angles other than 0˚ still have too much background to be clinically useful. We have discovered that when the beam angle is positive, the background light that is created by the fiber causes fluorescence in our scintillator crystal. This gave us an increase in signal, which is not what we wanted. The Cerenkov light that propagates to the crystal and is converted to the scintillator light through visible fluorescence is not filtered by the optical filter and will always cause for an unacceptable background with the configuration used here.

In Part 3-2, we rotated the system 90° so our crystal is now pointing towards the gantry. We repeat the experiment without filter and a gantry angle now in the range from -90° to 90°. The result of the green system showed us an oscillating response. This is because the dark counts are oscillating all the time, and therefore it will affect our result. But the error is within 2.5%. This is very acceptable. For the red system, we see there is a sudden change near angle 0°. The cause of this effect is suspect to be the cement between the crystal and the fiber is not uniformly laid. If the thickness of the cement is not 100% uniform throughout the joint surface of both fiber and scintillator, then this will affect the result. In our case, the error is about 10%.

Overall, this research experiment helped us understand the importance of scintillator crystal light output. From the Cerenkov spectrum, even though the amount of cerenkov is less in red compared to green, because of its low light output the red still can’t manage to give a better SOBR than the green. In the end, the green system took the winning flag.

There are still many areas in this experiment can be improved. The crystal we were using actually starts to heat up after a lot of MU exposure. This affects our result by giving us a higher response. In the future, if crystal manufactures manage to produce a new crystal with more heat resistance properties, this will definitely improve this experiment a lot.

A higher standard of shielding for the electronic components should be used. This will give us a better integration and signal accuracy. When assembling the system, more precise accuracy needs to be performed. For example when laying the cement on the crystal to attach to the fiber, the cement needs to be uniformly laid.

Lastly, this experiment is to be compared with Mohammad Ali Alhabdan's doctor of philosophy research project in the medical physics department of University of Canterbury, Christchurch, New Zealand. Mohammad used a blue emitting crystal with wavelength 425nm. Our red system does not out-perform Mohammad's blue crystal. But our green system did perform better than Mohammad's blue crystal. Blue crystal will give an even higher light output than the green, but background signal (Cerenkov) will increase too. Our result agrees with L. Archambault [1].

ACKNOWLEDGEMENTS

I would like to especially acknowledge Assoc. Prof. Lou Reinisch, Dean of Science, director of medical physics, department of Physics and Astronomy, Univeristy of Canterbury for his great supervision, encouragement and support.

I would like to acknowledge Mark Bird, senior medical physicist in CDHB for his great assistance during the practical work performed in the Christchurch Hospital.

I would like to thank two members from the workshop department, Graeme Kershaw, Head of mechanical workshop and Ross Ritchie, Head of electronics workshop for your wonderful work with the equipments.

This Research has been funded under the department of Physics and Astronomy, University of Canterbury.

Finally, I would like to thank Dr. Phil Butler, head of department, department of Physics and Astronomy, University of Canterbury and Graham Sorrel, Principle Physicist, department of Radiation Oncology, Canterbury District Heath Board (CDHB) Christchurch Hospital for your combine relation which allows the completion of this research Project.

REFERENCES

[1]L. Archambault, J. Arsenault, L. Gingras, A. S. Beddar, R. Roy, and L. Beaulieu, "Plastic scintillation dosimetry: Optimal selection of scintillating fibers and scintillators," Med Phys. 32, 2271-2278 (2005).

[2]M. A. Clift, P. N. Johnston, and D. V. Webb, "A temporal method of avoiding the Cerenkov radiation generated in organic scintillator dosimeters by pulsed mega-voltage electron and phone beams," Phys. Med. Biol. 47, 1421-1433 (2002).

[3]A. S. Beddar, "A new scintillator detector system for the quality assurance of ^{60}Co and high energy therapy machines," Phys. Med. Biol. 39, 253-263 (1994).

[4]J. Indra, M. J. Gazda, and A. S. Beddar, "Characteristics of a scintillator based daily quality assurance device for radiation oncology beams," Med. Phys. 23, 2061-2067 (1996).

[5]W. U. Laub and T. Wong, "The volume effect of detectors in the dosimetry of small fields used in IMRT," Med. Phys. 30, 341-347 (2003).

[6]B. L. Leybovish, A. Sethi, and N. Dogan, "Comparison of ionisation chambers of various volumes for IMRT absolute dose verification," Med. Phys. 30, 119-123 (2003).

[7]D. A. Low, P. Parikh, J. F. Dempsey, S. Wahab, and S. Huq, "Ionisation chamber volume averaging effects in dynamic intensity modulated radiation therapy beams," Med. Phys. 30, 1706-1711 (2003).

[8]J. T. Bushberg, J. A. Seibert, E. M. Leidholdt JR., and J. M. Boone, "The essential physics of medical imaging", Second Edition, Lippincott Williams & Wilkins, Philadelphia, PA 19106 USA, Page 641, 2002.

[9]M. A. Clift, R. A. Sutton, and D. V. Webb, "Dealing with Cerenkov radiation organic scintillator dosimeters by bremsstrahlung beams," Phys. Med. Biol. 45, 1165-1182 (2000).

[10]J. V. Jelly, Cerenkov Radiation and its applications (Pergamon, London, 1958).

[11]A. S. Beddar, T. R. Mackie, and F. H. Attix, "Water-equivalent plastic scintillation detectors for high-energy beam dosimetry: I. Physical characteristics and theoretical consideration," Phys. Med. Biol. 37, 1883-1900 (1992).

[12]A. S. Beddar, D. J. Mason, and P. F. O'Brien, "Absorbed dose perturbation caused by diodes for small field photon dosimetry," Med. Phys. 21, 1075-1079 (1994).

[13]A. S. Beddar, T. R. Mackie, and F. H. Attix, "Water-equivalent plastic scintillation detectors for high-energy beam dosimetry: II. Properties and measurements," Phys. Med. Biol. 37, 1901-1913 (1992).

[14]A. S. Beddar, T. R. Mackie, and F. H. Attix, "Cerenkov light generated in optical fibers and other light pipes irradiated by electron beams," Phys. Med. Biol. 37, 925-935 (1992).

[15]M. A. Clift, R. A. Sutton, and D. V. Webb, "Water equivalence of plastic organic scintillator in megavoltage radiotherapy bremsstrahlung beams," Phys. Med. Biol. 45, 1885-1895 (2000).

[16]T. O. White, "Scintillating fibers," Nucl. Instrum. Methods Phys. Res. A 273, 820-825 (1988).

[17]J. M. Fontbonne, G. Iltis, G. Ban, A. Battala, J. C. Vernhes, J. Tillier, N. Bellaize, C. LeBrun, B. Tamain, K. Mercier, and J. C. Motin, "Scintillating fiber dosimeter for radiation therapy accelerator," IEEE Trans. Nucl. Sci. 49, 2223-2227 (2002).

[18]H. Perera, J. F. Williamson, S. Monthofer, W. R. Binns, J. Klarman, G. L. Fuller, and J. W. Wang, "Rapid two-dimensional dose measurement in brachytherapy using plastic scintillator sheet: Linearity, signal to noise ratio and energy response characteristics," Int. J. Radiat. Oncol., Biol., Phys. 23, 1059-1069 (1994).

[19]D. Letourneau, J. Pouliot, and R. Roy, "Miniature scintillating detector for small field radiation therapy," Med. Phys. 26, 2555-2561 (1999).

[20]W. R. Leo, Techniques for Nuclear and Particule Physics Experiements, 2nd ed. (Springer-Verlag, New York, 1994).

[21]S. F. Boer, A. S. Beddar, and J. A. Rawlinson, "Optical filtering and spectral measurements of radiation-induced light in plastic scintillation dosimetry," Phys. Med. Biol. 38, 945-958 (1993).

[22]P. L. Mattern, L. M. Watkins, C. P. Skoog, J. R. Brandon, and E. H. Barsis, "The effects of radiation on absorption and luminescence of fiber optic waveguides and materials," IEEE Trans. Nucl. Sci. 21, 81-93 (1974).

[23]K. J. Jordon, "Evaluation of ruby as a fluorescent sensor for optical fiber based radiation dosimetry," Proc. SPIE 2079, 170-178 (1996).

[24]B. L. Justus, P. Falkenstein, A. L. Huston, M. C. Plazas, H. Ning, and R. W. Miller, "Gated fiber-optic-coupled detector for *in vivo* real-time radiation dosimetry," Appl. Opt. 43, 1663-1668 (2004).

[25]A. S. Beddar, N. Suchowerska, and S. H. Law, "Plastic scintillation dosimetry for radiation therapy: Minimising capture of Cerenkov radiation noise," Phys. Med. Boil. 49, 783-790 (2004).

[26]M. A. Alhabdam, "Dosimeters using plastic scintillators and fiber optics," University of Canterbury PhD thesis (2005).

APPENDIX

ELECTRONIC BOX

This is a photo of our electronics box. The yellow BNC socket is for the pulse trigger from the LINAC. At the top there are two sockets for channel 1 and channel 2 optical fiber input. The LED displays number of counts detected for channel 1 and 2. The reset button is to reset everything on LED to zero.

EXPERIMENT SET UP FOR PART 3-1 (Scintillator Crystal)

The following photos are showing the experiment set up for part 3-1. The hollow plastic square rod is suspended in air by using a metal clamp. The scintillator crystal exit from one end which is aimed at the iso-center.


X1
X2
CLINAC 600C

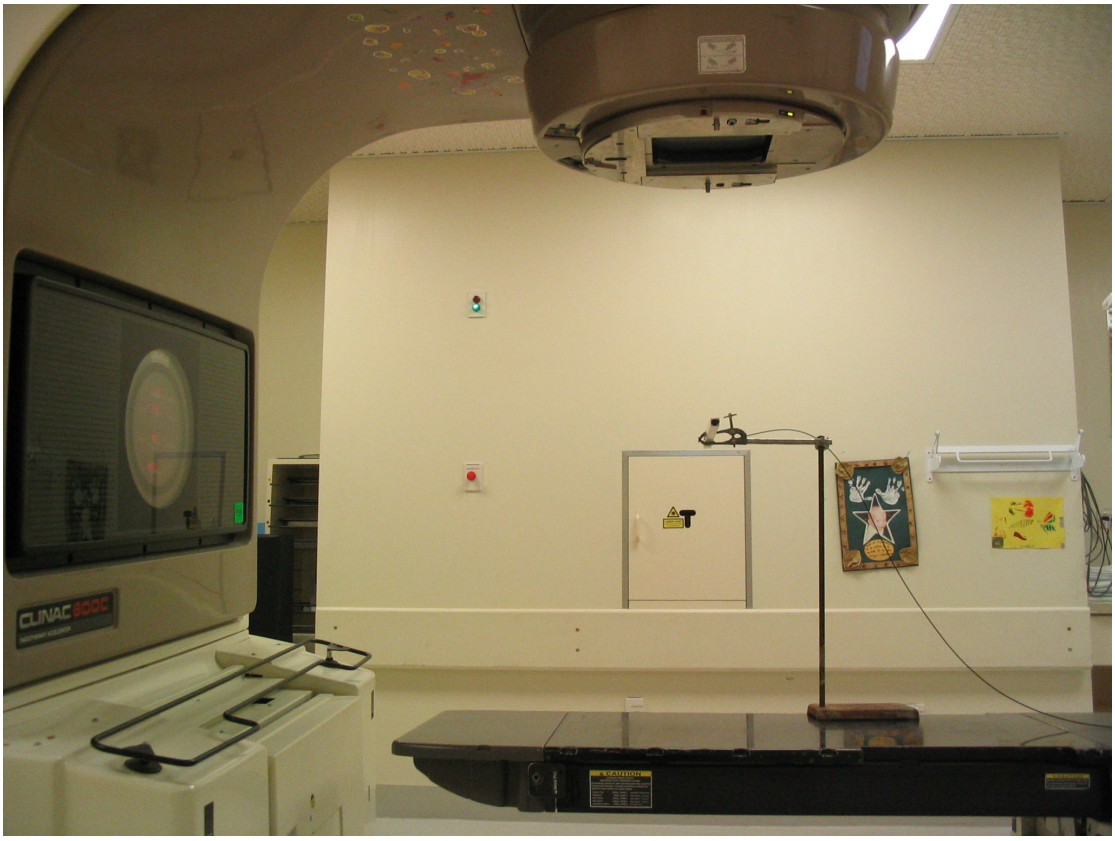
CLINAC 600C

EXPERIMENT SET UP FOR PART 3-1 (Fiber)

The following photos are showing the experiment set up for part 3-1. Now we can see to irradiate only the fiber, the fiber need to go through the hollow square rod and exit from the distal end. The scintillator crystal needs to be placed away from the iso-center (we allow 3 meters). We aim the iso-center near the middle of the plastic rod, so when we start to rotate the gantry to either side, we will always have flat uniform fiber lying inside the beam field.

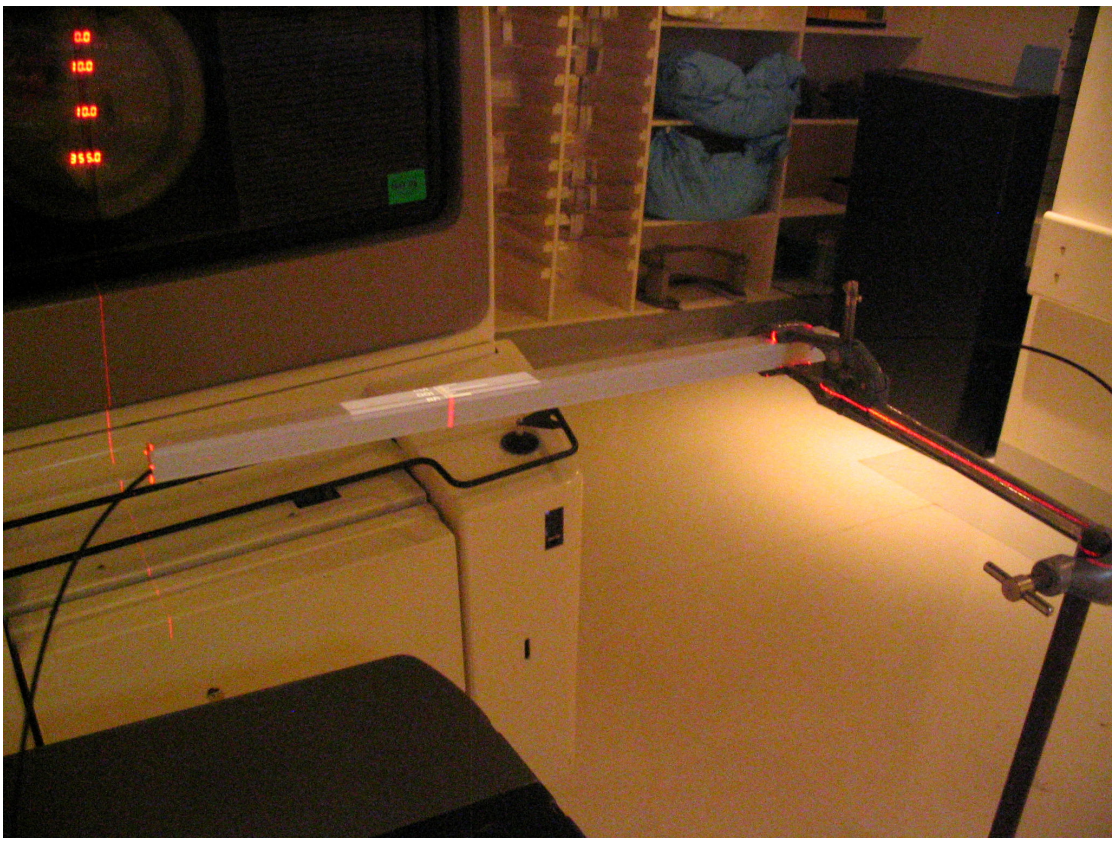


NAC 600C

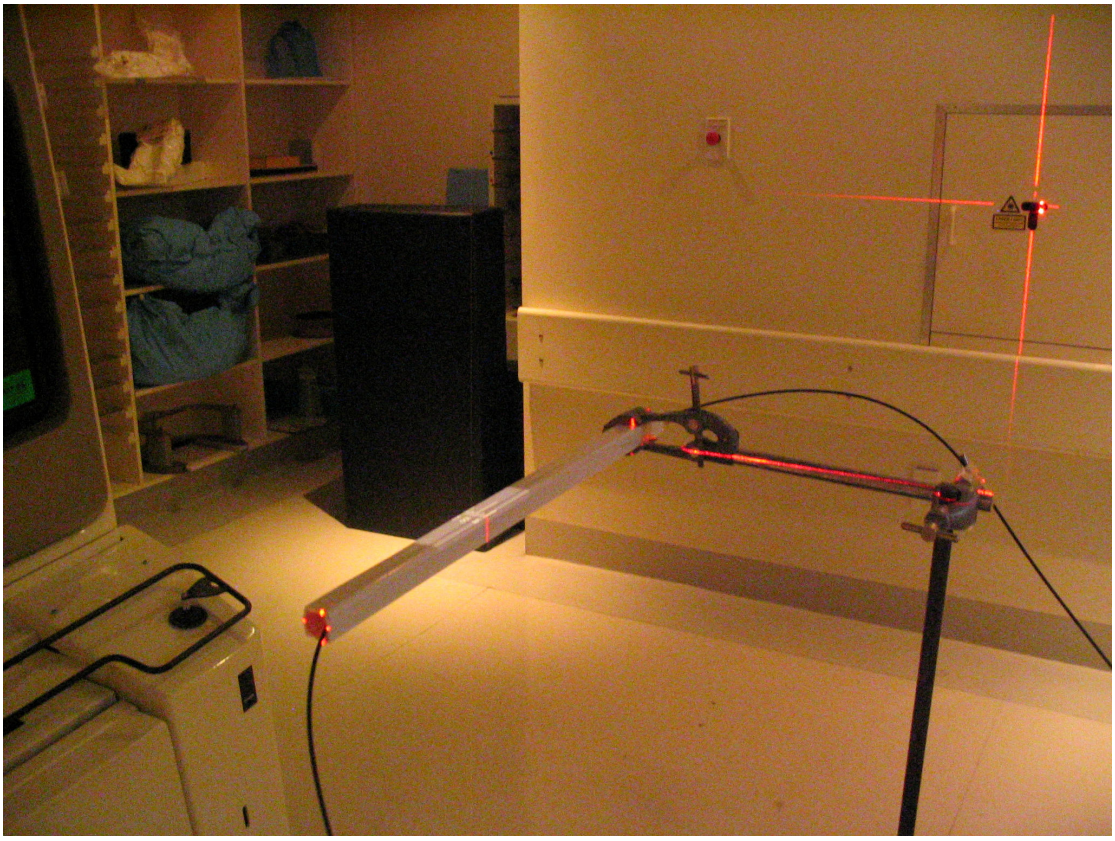

BLOCK DIAGRAM OF DOSIMETER ELECTRONICS

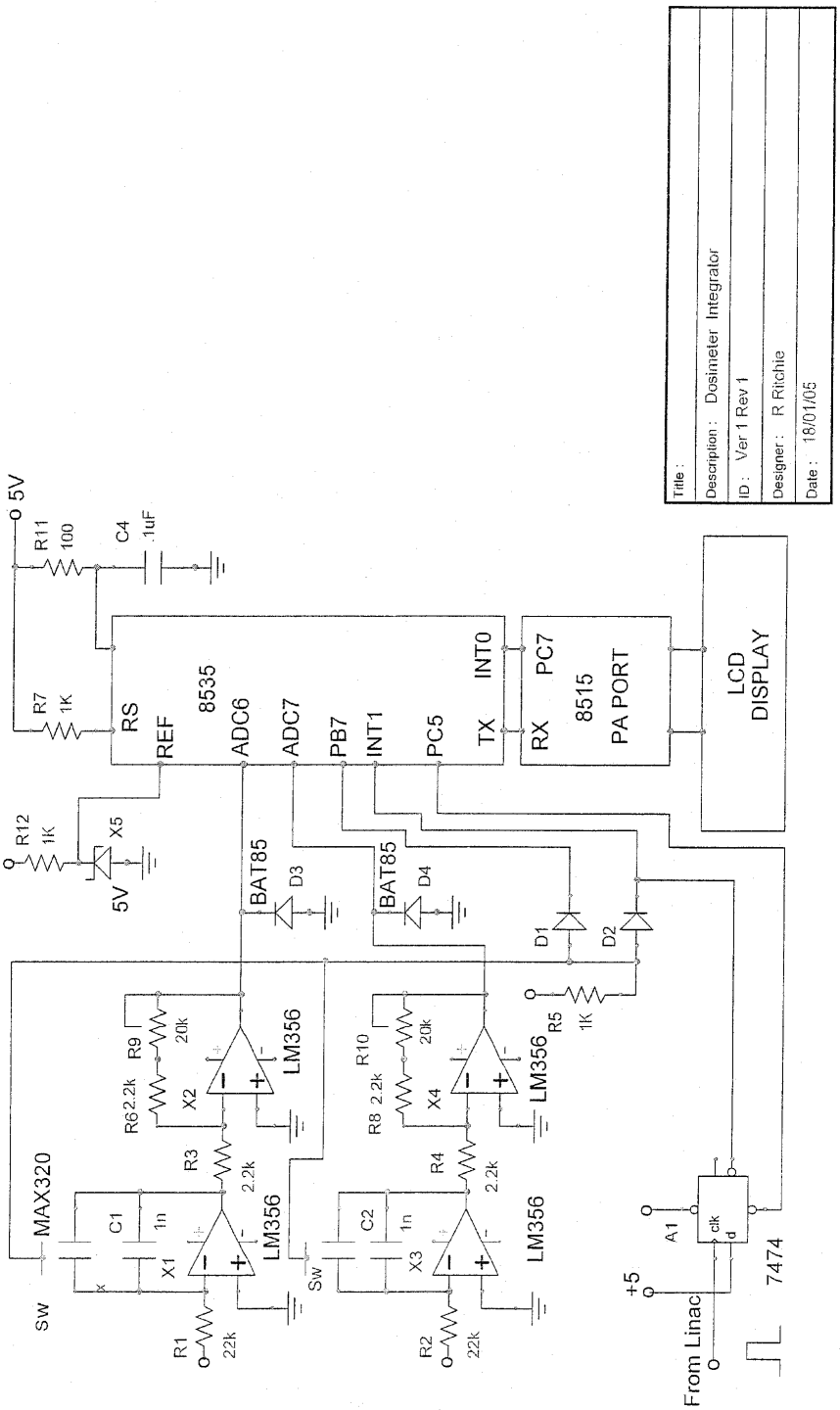

TIMING DIAGRAM OF DUAL INTEGRATOR SYSTEM